Development of a system for forest measurement in mountainous coniferous forests using small-footprint airborne LiDAR

Small-footprint 型航空機 LiDAR による山岳地域針葉樹林の森林計測システムの開発

Tomoaki TAKAHASHI
高橋與明

Contents

Tomoaki TAKAHASHI : Laboratory of Forest Environment and Resources, Graduate School of Bioagricultural Sciences, Nagoya University, Nagoya 464-8601, Japan
(Present Address : Department of Forest Management, Forestry and Forest Products Research Institute, Tsukuba 305-8687, Japan)
高橋與明：名古屋大学大学院生命農学研究科 森林環境資源学研究室（現：(独)森林総合研究所 森林管理研究領域）
（受理：2006年11月1日）

Chapter 1. Background

The Kyoto Protocol and small-footprint airborne LiDAR remote sensing

The Kyoto Protocol was adopted at the Third Conference Of the Parties (COP3) of the United Nations Framework Convention on Climate Change (UNFCCC) in 1997. The protocol calls for Annex I Parties (industrialized countries who have historically contributed the most to climate change) to limit or reduce their carbon equivalent emissions of greenhouse gases (GHGs) by 5.2% of their 1990 levels in the first commitment period (2008-2012) (Yamagata *et al.* 2001; Peter 2004; Gundimeda 2004). In the protocol, Japan committed itself to decreasing mean average carbon dioxide (CO_2) emission levels to 1.155 billion tons, a 6% decrease from the 1.229 billion tons CO_2 emitted in 1990 (Fujisawa 2004). During the COP7 conference, UNFCCC allowed Japan to sink 13 million tons carbon (or 47.67 million tons CO_2, 3.9 % of the gross emission rate in 1999) in forest; a percentage second only to that of Canada among Annex I states (Yamagata *et al.* 2002). Although the Kyoto Protocol permits signatories to employ carbon sinks, that is Article 3.3 and 3.4 activities, to achieve their respective emission reduction targets during this period, Annex I Parties are required to report emission by source and removal by sinks of GHGs resulting from land use, and land-use change and forestry (LULUCF) activities under Article 3.3 (afforestation (A), reforestation (R) and deforestation (D)), as well as selected human-induced activities under Article 3.4 (forest management (FM), revegetation (R), cropland management (CM), and grazing land management (GM)) that have occurred since 1990 (IPCC 2004). Although one of the largest allocations for carbon sink activities (3.9%) was endorsed to enable Japan to achieve the proposed reduction targets (6%), there are still numerous issues that need to be addressed regarding implementation of mechanisms necessary to meet this challenge. These include expanding the scope of FM, development of a carbon accounting system that considers ARD activities as they relate to FM activities and that can account for the amount of carbon in carbon sinks, and to verify the efficiency of carbon sinks (Yamagata *et al.* 2002; Matsumoto 2005).

In the protocol, FM is defined as a system of practices for the stewardship and use of forest land and is aimed at fulfilling the relevant ecological (including biological diversity), economic and social functions of a forest in a sustainable manner (IPCC 2004). Consequently, the number of properly managed forests capable of meeting these demands must be increased urgently in order to secure a large carbon sink (Matsumoto 2005). The identification of areas suitable for ARD and FM activities in a carbon accounting system is likely to involve the application of remote sensing techniques in carbon sink assessment. Such a system would have to meet the needs of the Kyoto Protocol and beyond, since the Kyoto Protocol mandates each country to report data on the monitoring of carbon sink activities in a transparent and verifiable manner for (Yamagata *et al.* 2001). Peter (2004) states that recent developments in remote sensing technology have increased the potential of this tool to monitor and assess the earth's surface, and that satellite or airborne remote sensing, with increased capabilities in terms of spatial, temporal and spectral resolution, allow more efficient and reliable monitoring of the environment over time at global, regional and local scales. Moreover, Rosenqvist *et al.* (2003) suggested that remote sensing is well suited to quantify changes in the environment in relation to LULUCF activities, and that a major benefit of applying remote sensing data to calculations of emissions is that many systematic observation systems are available and historical data archives exist that can be augmented through current and future data acquisitions.

To better facilitate the accounting of carbon sinks under Article 3.3 and 3.4 in Japan, Matsumoto (2005) recommended extensive use of forest registers and forest planning maps. This is because Japan does not have much space to implement AR activities and will thus have to depend mainly upon FM activities as described in Article 3.4, instead of ARD activities under Article 3.3, to sink 13 million tons of carbon (Yamagata and Ishii 2001; Matsumoto 2005). Consequently, detailed monitoring of FM activities is likely to be dependent on the compilation of accurate forest registers. Since forest registers and planning maps contain information on the attributes and geographic location of individual forest stands for the entire country, supplementing them with information contained in management records has the potential for accurate carbon sink assessments.

The development of a system for verifying the efficiency of the carbon sink is one of the most significant issues that need to be addressed. The Good Practice Guidance (GPG) for LULUCF state that monitoring requires that provisions be made for quality assurance (QA) and that quality control (QC) needs to be implemented by means of a QA/QC plan. The plan should form part of project documentation and cover the following procedures: (1) collecting reliable field measurements; (2) verifying methods used to collect field data; (3) verifying data entry and analysis techniques; and (4) data maintenance and archiving. If after implementing the QA/QC plan it is found that the targeted precision level is not met, then additional field measurements need to be conducted until the targeted precision level achieved. If Japan implements carbon sink accounting relying principally on the data contained in forest registers and planning maps, there exists the likelihood of large uncertainties in estimates of accounted carbon in the sink because of disparities between field and forest register (Encyclopedia of Forest and Forestry 2001). Therefore, especially for Japan, the verification system will need to be both objective and accurate in accordance with QA/QC plan.

Regarding the format of such a verification system, the GPG state that remote sensing is useful for verifying both changes in living biomass, and land use and land-use changes (IPCC 2004).

The two types of optical remote sensing sensors are currently in use are passive and active optical sensors. The former records naturally occurring electromagnetic radiation that is reflected or emitted from the objects of interest, while the latter bathes the objects in man-made electromagnetic energy and then records the amount of radiant flux returning to the sensor system (Jensen 1996). The passive optical remote sensing sensors, such as Landsat Thematic Mapper (TM) and Multi-Spectral Sensor (MSS), and SPOT High Resolution Visible (HRV) are most frequently used. Although a comprehensive discussion of remote sensing instruments appears in Jensen (1996), optical remotely sensed data from passive optical sensors are generally a result of a complex series of interactions between the electromagnetic radiation emitted by the sun that is reflected off the earth's surface and received by a sensor. In a forestry context, this complex series of interactions is affected by factors such as optical properties of the stand, spatial resolution (scale), stand object relationship to scale and spatial aggregation (Wulder 1998). Typically, passive optical sensors are only capable of providing detailed 2-D spatial data in the horizontal plane distributions as digital (or analog) optical imagery. This data, however, is not well suited to the representation of vertical data such as the vertical distribution of vegetation in forests. Wulder (1998) reviewed various passive optical remote sensing systems and techniques for the purposes of forest inventory and assessment of biophysical parameters in detail. Lefsky *et al.* (2001) evaluated alternate remote sensing products for forest inventory and monitoring. Although Leckie (1990) and Leckie *et al.* (1995) stated that, while current technological developments have facilitated greater spectral and spatial resolution on a variety of platforms and that this has enabled remote measurement of forest inventory parameters, the collection of detailed and accurate information of vertically distributed forest attributes, such as stand height and volume, acquired with passive optical sensors is limited by the technical capabilities of extant remote sensing instruments (St-Onge *et al.* 2003). Consequently, passive optical remote sensing techniques are considered most suitable for assessments of specific forest areas and to manage ARD activities (Sekine *et al.* 2002) provided that ground reference data is available (IPCC 2004).

On the other hand, remote sensing techniques that generate both horizontal and vertical (3-D) data is a promising and fast growing field, and some techniques have proved more accurate than spectral remote sensing for certain applications (Hyyppä *et al.* 2000; Lefsky *et al.* 2001). In recent years, the Light Detection And Ranging (LiDAR) remote sensing technique, an active remote sensing technique, has recently received considerable interest owing to its ability to accurately measure the shape and height of objects with a high special resolution. LiDAR is capable of providing both horizontal and vertical information with feasible sampling density that is dependent on the types and configurations of LiDAR system (Lim *et al.* 2003). The most remarkable attribute of LiDAR is that it does not receive the reflectance spectra of objects as produced using passive optical sensors, but rather, data is presented as the three coordinates (*X*, *Y*, *Z*) of the objects of interest directly, accurately and precisely. Particularly important is the ability of LiDAR to measure the height of an object more accurately than is possible using passive optical sensors (Kraus and Pfeifer 1998).

A LiDAR system typically consists of a platform (e.g., helicopter or aircraft) and a scanning laser sensor that measures the roundtrip time for a pulse of energy to travel between the sensor and a target. The elapsed time from when a laser is emitted to when it intercepts with an object and then is registered by the sensor can be measured using either (1) pulsed ranging, where the travel time of laser pulse from a sensor to a target object is recorded; or (2) continuous wave ranging, where the phase change in a transmitted sinusoidal signal produced by a continuously emitting laser is converted into travel time (Lim *et al.* 2003). The former and the later systems are referred to as small-footprint and large-footprint LiDAR, respectively (Fig 1-1). Here, footprint means the circular area on the surface of an object that is covered by the laser at a moment in time and is represented in Fig 1-1. Most modern small-footprint systems

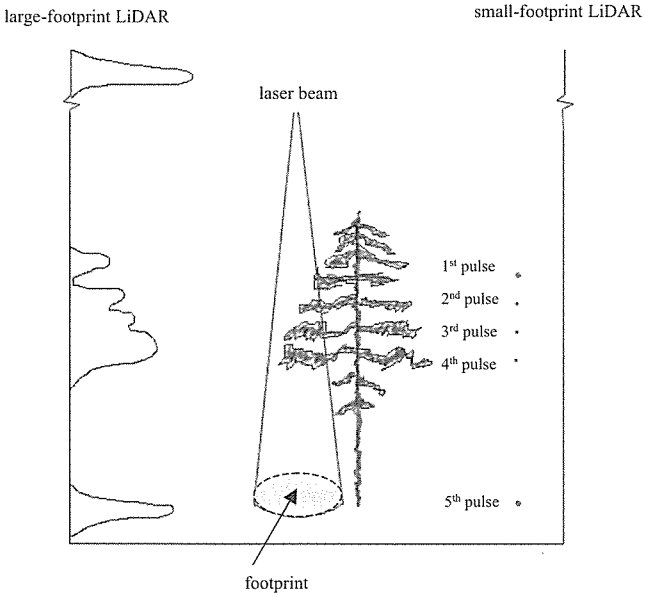

Fig 1-1. Differences between discrete return (small-footprint) and waveform (large-footprint) vertical sampling. The 1st to 5th pulse points refer to the returning pulse. This figure is a modification from Lim *et al.* (2003).

(typically with a diameter less than 1 m) can discriminate between multiple laser returns from the same laser pulse based on the intensity and time of arrival (Hodgson *et al.* 2003). Such discrete LiDAR systems typically only record the occurrence of the first and last returns from a series of returns corresponding to discrete surfaces along the slant angle (St-Onge *et al.* 2003). The first and last laser returns from the same laser pulse are referred to as the first pulse and the last pulse, respectively. Knowledge of the position of the sensor from the collected data using an onboard Global Positioning System (GPS) and Inertial Navigation System (INS), the distance from the sensor to a target, and the incident angle of each laser pulse, means that the three coordinates (*X*, *Y*, *Z*) of objects reflected within a footprint can be easily calculated. Small-footprint LiDAR remote sensing techniques have been anticipated as potentially useful for reducing fieldwork such as for estimating tree height (Means *et al.* 2000; Yamagata *et al.* 2002). Unlike the many small-footprint airborne LiDAR systems offered by commercial operators (Evans *et al.* 2001; St-Onge *et al.* 2003), the large-footprint (10-25 m) LiDAR systems that have been used successfully in studies of forest characteristics (Means *et al.* 1999), are only operated by large agencies such NASA and are not available on a commercial basis.

Small-footprint airborne LiDAR remote sensing techniques have shown considerable potential for detailed forestry monitoring. The technique has been used for estimating mean tree height since the mid 1980s, and has provided accurate canopy height estimates. Initially, these fast small-footprint LiDAR systems could only record reflections from a single track along a flight path (Maclean and Krabill 1986; Nelsson *et al.* 1988; Jensen *et al.* 1987; Ritchie *et al.* 1992, 1993; Rignot *et al.* 1994), but the development of scanning LiDAR sensors meant that both horizontal and vertical information on forest structure could be acquired. However, the fast scanning LiDAR systems where only capable of low sampling rates and this caused large underestimations of stand height because of failure to sample the tops of canopy trees (e.g., Nilsson 1996; Næsset 1997a). Subsequently, the sampling rate of small-footprint airborne LiDAR systems has progressed enormously and the technology of platform positioning has also greatly improved. Many of the recent commercial small-footprint airborne LiDAR systems, as listed in Baltsavias (1999b), have high sampling rates and the ability to provide accurate 3-D coordinates (*X*, *Y*, *Z*) of objects and can measure and estimate individual tree height, crown diameter, stem diameter and stem volume - all significant factors for estimating biomass - and can be used to account for carbon stock, accurately in boreal coniferous forests with flat terrain and low canopy closure (Hyyppä and Inkinen 1999; Hyyppä *et al.* 2001; Persson *et al.* 2002). Consequently, if accurate and detailed forest measurements and monitoring can be done in Japan by small-footprint airborne LiDAR, we may be able to apply the technique to checking the amounts of carbon stock accounted for in sinks on regional scale in a transparent and verifiable manner in accordance with QA/QC plan under the Kyoto Protocol. Airborne remote sensing techniques can also reduce the costs and time associated with conducting forest inventories compared to if it is done completely by field crews on regional scale.

However, detailed research on the application of small-footprint airborne LiDAR to forest measurements in Japan is limited to the study of Yone *et al.* (2002) for middle-aged Japanese larch (*Larix leptolepis*) plantations in flat terrain, and Omasa *et al.* (2003) for middle-aged sugi (*Cryptomeria japonica* D. Don) plantations in flat terrain and low stand density (approximately 873 trees/ha). The forest areas for FM activities under the Kyoto Protocol in Japan are likely to be mainly coniferous forests rather than broad-leaved forests, because of the faster growth of the former (Matsumoto 2001). Approximately 40% (ca. 10 million ha) of the forested area (25 million ha) in Japan consists of coniferous plantations of young to middle-aged sugi and hinoki cypress (*Chamaecyparis obtusa* Sieb. et Zucc.) (Japan Forestry Association 2003). In addition, many denser coniferous forests consisting of these species that have not been adequately thinned and weeded in mountainous areas exist. The topography of these areas is likely to be steeper and more complex than that of previously studied sites. Consequently, if the intended application is for cross-checking of the carbon stock accounted for, and assessing the extent of the carbon sink and planning FM activities, then we must demonstrate the potential of small-footprint airborne LiDAR to measure and monitor dense mountainous forests because no detailed research has been conducted in these areas. We therefore decided to conduct small-footprint airborne LiDAR in mountainous coniferous forests in this study.

Objective

The goal of this study was the development of a system for forest measurement in mountainous coniferous forests - mainly middle-aged sugi and hinoki cypress plantations in Japan - using small-footprint airborne LiDAR. Particularly, the accurate determination of tree height was considered particularly important as it is one of the most significant parameters in forest measurement. It is widely known that tree height is closely related to site quality and that this is an important indicator of forest productivity and fertility. Consequently, accurate tree height estimates can be used to infer site quality. In addition, tree height is a useful parameter for estimating the stem volume and the stand volume, both of which are required to account for carbon stock and sink. However, the measurement of tree height by field crews is very expensive and time consuming. It is also difficult to acquire accurate tree height measurements using field crews on steep slopes in mountainous areas. There should therefore be considerable incentive to investigate the potential for application of small-

footprint airborne LiDAR to estimate tree height as part of developing a system of forest measurement accurately in mountainous forests.

Principally, tree height estimates using small-footprint airborne LiDAR data are calculated by subtracting the estimated ground elevation from the outer layer of canopy vegetation. Kraus and Pfeifer (1998) demonstrated the inverse relationship that exists between large the slope angle decreased accuracy of LiDAR-derived bare ground height (i.e., Digital terrain Model; DTM) in Vienna Woods. Given the lack of sufficient evidence into whether DTMs and tree height can be estimated accurately in mountainous forests, we shall first examine the possibility of creating DTMs with accurate tree height estimates within sugi and hinoki cypress stands in Chapter 2. After considering the results in Chapter 2, we will then explore useful methods for forest measurement in hinoki cypress and sugi stands in Chapters 3 and 4, respectively. These methods are then summarized as a system for forest measurement in mountainous coniferous forests using small-footprint airborne LiDAR in Chapter 5, where current issues relating to small-footprint airborne LiDAR applied to forest measurements and future issues of Kyoto Protocol are also discussed.

Chapter 2. The penetration rate of laser pulse transmitted from a small-footprint airborne LiDAR in a middle-aged pure sugi (*Cryptomeria japonica* D. Don) and hinoki cypress (*Chamaecyparis obtusa* Sieb. et Zucc.) plantation

Introduction

Since the mid 1980s, the application of small-footprint airborne Light Detection And Ranging (LiDAR) remote sensing techniques, particularly for estimating individual tree height and stand canopy height have been studied by many researchers. Most modern small-footprint (typically less than 1 m in diameter) LiDAR sensors, as listed in Baltsavias (1999b), can discriminate between multiple laser returns from the same laser pulse based on the intensity and time of arrival (Hodgson *et al.* 2003). The first and last laser returns from the same laser pulse are referred to as the first pulse and the last pulse, respectively. Knowledge of the position of the sensor from the collected data by using an onboard Global Positioning System (GPS) and Inertial Navigation System (INS), the difference between the sensor and a target and the incident angle of each laser pulse, enables easy calculation of the three coordinates (X, Y, Z) of objects reflected within a circular laser spot (i.e., footprint).

Previous researches revealed the potential of small-footprint airborne LiDAR to measure and estimate individual tree height with an accuracy in the range of one meter in some types of coniferous forests (e.g., Hyyppä and Inkinen 1999; Hyyppä *et al.* 2001; Persson *et al.* 2002; Yone *et al.* 2002; Omasa *et al.* 2003). In order to obtain tree heights using small-footprint airborne LiDAR data (i.e., 3D point clouds), Digital Terrain Model (DTM), which represents the elevation of bare ground surface is required since tree height estimation is generally achieved by subtracting a DTM from a Digital Surface Model (DSM), which represents the elevation of the outer vegetation layer of a forest canopy. In other words, since the quality of DTM affects the tree height estimates (e.g., Hyyppä *et al.* 2004), the generation of accurate DTM is important.

Hyyppä *et al.* (2004) have suggested that in addition to the errors caused by applied LiDAR systems, methodology and algorithms for creating DTM (e.g., Kraus and Pfeifer 1998; Axelsson 1999; Elmqvist 2000; Brovelli *et al.* 2004), the quality of DTM derived from LiDAR data is influenced by data characteristics (e.g., measurement density, first/last pulse, flight height and scan angle), as well as errors due to characteristics of the complexity of target, i.e., type of terrain, flatness of terrain, density of the canopy etc. The factors that can be considered to influence the quality of the DTM would include the suggestion mentioned above, the fact that DTM should ideally be derived from LiDAR pulse data that hits the bare ground surface and the penetration rates, i.e., the percentage of the pulses that hit the ground within forests.

Although the details of the study area were not provided (i.e., tree species, stand characteristics, etc.), Takeda (2004) suggested that many LiDAR pulses had not reached the ground surface in some areas within dense forests in Japan. In Japan, there exist many dense middle-aged (40-50-year-old) hinoki cypress (*Chamaecyparis obtusa* Sieb. et Zucc.) and sugi (*Cryptomeria japonica* D. Don) plantations that have not been adequately thinned. Therefore, prior to creating a DTM with an algorithm presented by previous researchers, we should first investigate the number of LiDAR pulses that can hit the ground in dense forests. In this study, we have investigated the penetration rates of LiDAR pulses in the pure middle-aged hinoki cypress and sugi stands that had not been adequately thinned and have compared the penetration rates between the two stands.

Materials and methods

Study area

The study area was the Nagoya University experimental forest located at the Aichi Prefecture in central Japan (lat. 35°12' N, long. 137°33' E, 930 m a.s.l.). A middle-aged pure sugi (48-year-old) and hinoki cypress (46-year-old) stand that had not been adequately thinned were chosen for this study because they are representative of several such plantations in Japan. Further, those areas of sugi and hinoki cypress stands were specifically chosen, where forest floor was covered with limited understorey vegetation. The topography of the sugi stand was a gentle slope

Table 2-1. Summary of plot reference data

Characteristic	Hinoki cypress stand	Sugi stand
Stem density (per ha)	3100	2500
Diameter at breast height (cm)[a]	10 – 24 (ave[d]. 16)	12 – 44 (ave[d]. 22)
Tree height (m)[b]	12.7 – 15.5 (ave[d]. 14.0)	20.4 – 25.9 (ave[d]. 22.6)
Crown base height (m)[b]	8.0 – 9.7 (ave[d]. 8.8)	12.2 – 15.3 (ave[d]. 14.1)
Increments in tree height[c]	1.030	1.021
Canopy openness (%)[c]	4.3	3.9

[a]For all trees within each plot

[b]For predominant trees within each plot

[c]Increments in tree height between 2001 and 2003 for two sample trees within each stand

[d]Ave. denotes average

[c]Grade of canopy openness was computed by hemispherical photography

and included the site, as shown in Takahashi *et al.* (2000), where random micro-topographies existed. The terrain of the hinoki cypress stand was a smoothed gentle slope.

During winter in 2003, i.e., after the growth season had ended, tree measurements were completed. First, a 10 × 10 m square plot was established within each stand. The diameter at breast height (DBH) for all trees was measured with a calliper, subsequently the tree height and crown base height for the trees with a larger average DBH were measured using a dendrometer within an accuracy of 1 cm (Ledha-Geo, Jenoptik laser, Jena, Germany), within each plot. Since there was an approximate two-year gap between the acquisition time of the LiDAR data (summer 2001) and the ground truth data, the stem analysis was performed on two sample trees (dominant and co-dominant trees) for each sugi and hinoki cypress stand, specifically to ascertain the increment in tree height during the two-year period. The arithmetic mean value of the increment in height for the trees was then deducted from the field measured tree heights and crown base heights within each stand. The corrected data was defined as field data and subsequently used for analysis in this study. A summary of the plot reference data, including the increment in tree height within each stand, is listed in Table 2-1.

LiDAR pulse data

The LiDAR pulse data acquisition was performed on August 17, 2001, using a helicopter-borne laser scanner operated by Nakanihon Air Service Co., Ltd., Japan. The pulsed laser beam moved across the helicopter track controlled by a scanner and along the track through the forward motion of the helicopter. The resulting pattern on the ground was thus Z-shaped. In this study, the position of the reflecting object was determined from only the first and second pulse. In this study, we considered second pulses as last pulses. Laser measurements were performed on a single flight line. The settings of the LiDAR system used in this study are shown in Table 2-2.

To select the LiDAR pulse data within each stand, geometrically corrected digital orthophotography was used in this study area. Aerial photographs acquired in October 2001 were converted into orthophotographs by Tamano Consultants Co., Ltd., Japan. The stand boundaries of the sugi and hinoki cypress stand in the study area were delineated on a computer using Geographic Information System (GIS), subsequently the delineated image was printed on papers and the boundaries were checked in the field. Since St-Onge *et al.* (2003) have mentioned that in order to maximize LiDAR pulse energy penetration through vegetation cover to the ground level, it is preferable to limit incidence angles to 15-20° off nadir, the LiDAR pulse data having an incidence angle less than approximately 15° within each stand was selected and used in the analysis. Subsequently, the stand area used for the analysis was 4,800 m^2 for each stand and the 10 × 10 m plot mentioned above was included within each area.

Table 2-2. Settings of the LiDAR system

Parameter	Performance
Laser pulse frequency	20,000 Hz
Scan frequency	24 Hz
Scan angle	±30°
Beam divergence	0.5 mrad
Flying speed and altitude	43 km/h, 300 m
Footprint diameter	0.15 m
Measurement density[a]	4.76 points/m^2

[a]Theoretical number of transmitted laser pulses per square meter

Data analysis

In order to calculate the penetration rate, i.e., the percentage of the number of pulses that hit the ground, the LiDAR pulse data within each stand was divided into two groups. One was the LiDAR pulse data that was considered as having hit the ground and the other was the LiDAR pulse data that was considered as having hit non-ground, i.e., vegetation. To investigate the number of pulses that hit the ground, a referential DTM (DTM_{ref}) was first created as datum surface in order to select these pulses. Since

Takahashi *et al.* (2000) suggested that a continuous surface model passing through the predominant tree tops could reflect the ground surface at least in a small area, we first created a continuous surface model (hereafter, referred to as *top surface model* in this study) that passed only the LiDAR data that hit the tree tops within each stand. The procedures for creating the top surface model were as follows. First, the LiDAR pulse data that was considered to represent the tree top (i.e., local maxima) was selected using local maximum filtering that has been used in many previous studies for identifying tree locations using small-footprint airborne LiDAR data (e.g., Holmgren *et al.* 2003a; Hyyppä *et al.* 2001; Maltamo *et al.* 2004; McCombs *et al.* 2003; Popescu *et al.* 2002, 2003; Zimble *et al.* 2003). In order to avoid selecting local maxima within canopy gaps, i.e., bare ground area between tree crowns, our software named LiDAS (LiDAR Data Analysis System) which has the ability to identify individual canopy gaps, segment tree crowns, etc., was used for selecting only the local maxima within tree crowns. The top surface model was then created by spline interpolation (Magnussen and Boudewyn 1998; Magnussen *et al.* 1999; Riaño *et al.* 2003; Brovelli *et al.* 2004) using only the selected local maxima using GIS. Subsequently, the DTM_{ref} was created by subtracting the field mean canopy tree height from the surface model for each stand (Table 2-1).

Then the difference between the height of each LiDAR pulse data and the DTM_{ref} was calculated. If this difference was small, the pulse was regarded as having hit the ground. Conversely, if the difference was large, the pulse was regarded as having hit vegetation. In order to divide the LiDAR pulse data into two groups (i.e., ground and vegetation data) in each stand, we identified a threshold value from the histogram. In order to determine the threshold value, the mode method of thresholding was applied (Suematsu and Yamada 2000), i.e., the mode of the trough between the first and second peak in the histogram of each stand was selected as the threshold. For the purpose of this study, the LiDAR pulse data wherein the difference was less than the threshold value was defined as data for the pulses that hit the ground, and the LiDAR pulse data wherein difference was more than the threshold value was defined as the data for the pulses that hit the vegetation.

Subsequently, the penetration rate (P_{f+s}: %) was calculated as the percentage of pulses that hit the ground for each stand, as follows.

$$P_{f+s}=\left(\frac{N_{fg+sg}}{N_f}\right)\times 100 \quad (2\text{-}1)$$

where N_{fg+sg} and N_f are the number of pulses that hit the ground and the transmitted pulses from airborne LiDAR, respectively. Moreover, since the pulses that hit the ground (N_{fg+sg}) included both the first and second pulse, the penetration rate of the first pulse (P_f : %) and the second pulse (P_s : %) that hit the ground was also calculated for each stand, as follows

$$P_f=\left(\frac{N_{fg}}{N_f}\right)\times 100 \quad (2\text{-}2)$$

$$P_s=\left(\frac{N_{sg}}{N_f}\right)\times 100 \quad (2\text{-}3)$$

where N_{fg} and N_{sg} are the number of the first and second pulse that hit the ground, respectively. Additionally, the average area occupied by the data for one pulse that hit the ground was calculated with P_{f+s} for each stand to discuss the possibility of creating an accurate DTM. Finally, significant difference between these penetration rates of sugi and hinoki cypress stands was investigated by a statistical significance test for the difference between the two population proportions.

Results

Although, the theoretical number of the transmitted pulses with the LiDAR settings used in this study was 47,600 points/ha (Table 2-2), the actual number was greater than the theoretical value: 107,427 points/ha (hinoki cypress stand) and 122,883 points/ha (sugi stand). The threshold values for dividing LiDAR pulse data into the two groups, i.e., ground hits and vegetation hits were 2.5 m in the hinoki cypress stand and 4.5 m in the sugi stand, respectively, by the mode method of thresholding (Fig 2-1) and the penetration rate of the total pulses that hit ground (P_{f+s}) was 1.1 % and 8.1 % in the hinoki cypress and the sugi stands, respectively (Table 2-3). Also, the average area occupied by the data for one pulse that hit the ground was 8.5 m^2 and 1.0 m^2, respectively (Table 2-3). A sample of the LiDAR pulse data that hit vegetation and ground for each stand is shown in Fig 2-2. Moreover, the penetration rate of first the pulses that hit the ground (P_f) was one tenth of that of second pulses (P_s) in hinoki cypress stand and about a half in sugi stand (Table 2-3). According to a statistical significance test for the difference between the two population proportions, there was a significant difference for all penetration rates (i.e., P_{f+s}, P_f, and P_s) between the sugi stand and the hinoki cypress stand ($p < 0.001$).

Discussion

In this study, we have investigated the penetration rates, i.e., the percentage of the number of pulses that were considered as having hit the ground within an even-aged pure sugi stand and a hinoki cypress stand. To divide the LiDAR pulse data into ground data and vegetation data, we used DTM_{ref} created by using local maxima of the LiDAR pulse data and the field mean canopy height. According to Takahashi *et al.* (2000) who had studied a part of the area used in this study, the elevation of the tops of the predominant trees within a 30 × 35 m plot was regressed against the ground elevation of the bottom of the standing trees and the slope of the regression equation ($R^2 = 0.79, p < 0.01$) was 1.02. In addition, the detected tree tops (i.e., local maxima) obtained from

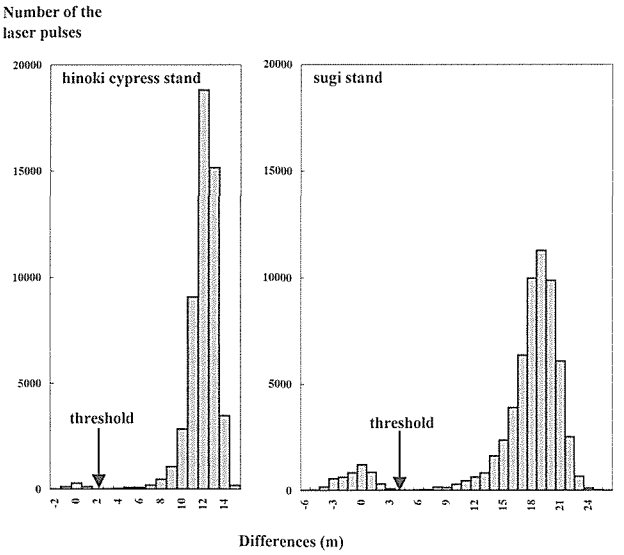

Fig 2-1. The histogram of the difference between the height of each LiDAR pulse data and a referential Digital Terrain Model (DTM_{ref}) within the hinoki cypress (*Chamaecyparis obtusa* Sieb. et Zucc.) stand (left) and sugi (*Cryptomeria japonica* D. Don) stand (right). The threshold was determined by the mode method of thresholding and the value was 2.5 m in the hinoki cypress stand and 4.5 m in the sugi stand. The class interval was 1 m.

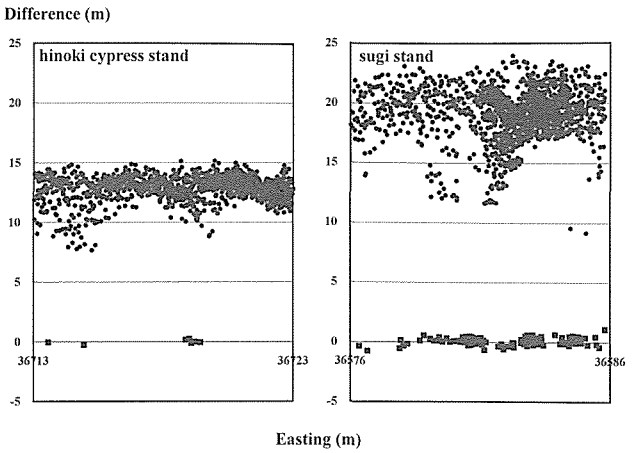

Fig 2-2. A sample vertical projective plane of LiDAR pulse data within a 10×10 m area extracted from the hinoki cypress (*Chamaecyparis obtusa* Sieb. et Zucc.) stand (left) and the sugi (*Cryptomeria japonica* D. Don) stand (right), within this study area. Black dots and squares denote LiDAR pulse data for hits on the vegetation and ground, respectively. Y-axis denotes the difference between the height of each LiDAR pulse data and a referential Digital Terrain Model (DTM_{ref}).

Table 2-3. Number of transmitted laser pulses and the penetration rate

Stand	Number of transmitted pulses per hectare and per square meter	Penetration rate (%)[a] P_{f+s}[b]	P_f[b]	P_s[b]	S (m^2)[c]
Hinoki cypress	107,427 points/ha (10.7 points/m^2)	1.1	0.1	1.0	8.5
Sugi	122,883 points/ha (12.3 points/m^2)	8.1	2.6	5.5	1.0

[a]Percentage of the number of the pulses that hit the ground

[b]F and s denote first and second pulse, respectively

[c]The average area for one pulse that hit the ground

small-footprint airborne LiDAR data by using local maximum filtering practically would belong to the canopy (i.e., predominant) trees (e.g., Persson *et al.* 2002; Yone *et al.* 2002), therefore the procedure for creating the DTM_{ref} presented in this study was considered to be suitable and the DTM_{ref} was used for dividing the LiDAR pulse data into ground and vegetation data. Fig 2-2 clearly shows vegetation data and ground data divided, and similar vertical projective planes of LiDAR pulse data, which shows definite vegetation data and ground data, have been presented in some previous researches (e.g., Brandtberg *et al.* 2003; Hirata *et al.* 2003; Riaño *et al.* 2003).

Penetration rate of the first pulse that hit the ground (P_f) in hinoki cypress stand was much lower than that of sugi stand and there were significant difference between the two population proportions (Table 2-3). This indicates that, although the degree of crown closure was not measured, there might have existed canopy gaps having sizes larger than the footprint size (i.e., approximately 0.15 m diameter in this study), or more gaps within a sugi stand than a hinoki cypress stand in this study area since P_f refers to the percentage of the number of the pulses that reached the ground directly without being prevented by the foliage and branches of crowns. Moreover, the penetration rate of the second pulse that hit the ground (P_s) in the hinoki cypress stand was only 1.0%. Considering the fact that light intensity on the floor of unthinned hinoki cypress plantations is so low that there is scarcely any understorey vegetation. (e.g., Hattori *et al.* 1992), the low penetration rate of LiDAR pulses may be attribute of the dense hinoki cypress stands.

As a result, the penetration rates of the total pulses that hit the ground (P_{f+s}) in this study were 1.1% in the hinoki cypress stand and 8.1% in sugi stand (Table 2-3), moreover, significant differences existed between the two population proportions. In

this study, considering the results of the number of transmitted pulses from airborne LiDAR (N_t) and P_{f+s}, the average area occupied by one pulse data that hit the ground was found to be approximately 8.5 m^2 in hinoki cypress stand and 1.0 m^2 in sugi stand (Table 2-3). This indicates that there is a possibility of creating a DTM theoretically with spatial resolutions of approximately 3 m and 1 m. However, as shown in Fig 2-2, particularly in the case of the hinoki cypress stand, the pulse data that hit the ground exhibited unevenness. Therefore, the accuracy of such a theoretical DTM may be considered to be low. Moreover, although the N_t per hectare was approximately twice the theoretical value (i.e., 47,600 points/ha) for this study area, the lower sampling density led to a reduced pulse data for the ground hits, and this has resulted in an inaccurate or low resolution DTM that cannot be considered reliable enough to estimate tree heights. Therefore, even if we use methodologies and algorithms for creating a DTM, as have been presented by previous researchers (e.g., Kraus and Pfeifer 1998; Axelsson 1999; Elmqvist 2000; Brovelli *et al.* 2004), it may be difficult to create an accurate DTM, especially in dense hinoki cypress stands as is used in this study, based solely on the information of the poorly penetrated LiDAR pulses that hit the ground.

Thus, the penetration rate of small-footprint airborne LiDAR pulses would significantly differ between even-aged improperly managed hinoki cypress and sugi stands in Japan. According to previous researches, stand conditions such as the stand age, tree species distributions, number of stems (Næsset and Bjerknes 2001; Næsset and Økland 2002; Næsset 2002), season, i.e., full-leaf and leafless season (Hirata *et al.* 2003) and extent of canopy closure (Cowen *et al.* 2000) could affect the penetration rate of the LiDAR pulses. Therefore, the penetration rates for various types and conditions of forests should be investigated in detail in order to create an accurate DTM and finally achieve accurate tree height estimation. Moreover, although we used a small-footprint helicopter-borne LiDAR system with only one setting as shown in Table 2-2 for the purpose of this study, other LiDAR settings (e.g., lower flying altitude and slower flying speed) or systems (e.g., smaller footprint, higher measurement density and more intense pulse energy), need to be investigated as suggested by Hyyppä *et al.* (2004), particularly for hinoki cypress stands with different stand conditions and new methodology and algorithms for creating accurate DTM will be required for estimating tree heights if the low penetration rates of LiDAR pulses within hinoki cypress stands are not improved by trying out other LiDAR settings.

Chapter 3. Forest measurement in hinoki cypress (*Chamaecyparis obtusa* Sieb. et Zucc.) plantations by small-footprint airborne LiDAR: Stand volume estimation

Introduction

Small-footprint airborne LiDAR has been used for estimating mean tree height or stand volume since the mid 1980s (Maclean and Krabill 1986; Nelsson *et al.* 1988; Jensen *et al.* 1987; Ritchie *et al.* 1992, 1993; Rignot *et al.* 1994) and some useful procedures for estimating of aboveground biomass or stand volume have been reported (Nilsson 1996; Næsset 1997b). Recently, Hyyppä and Inkinen (1999) estimated stand volume using LiDAR-derived individual tree height and crown area calculated with both first and last pulse data, and showed stand volume could be estimated with an R^2 value of 0.883. Means *et al.* (2000) estimated stand volume using LiDAR-derived predictor variables associated with canopy height and stand basal area calculated with both first and last pulse data, and estimated stand volume with R^2 values of 0.95 and 0.97. Persson *et al.* (2002) estimated stem volumes of 138 trees using LiDAR-derived individual tree height and LiDAR-estimated stem diameter calculated with both first and last pulse data, and showed stem volume could be estimated with r-value of 0.94.

In most of the studies mentioned above, a Digital Terrain Model (DTM) was calculated in order to compute the height above ground of each point as the difference between the first pulse, i.e., the elevation of canopy surface, and the last pulse, i.e., the ground surface height. But Kraus and Pfeifer (1998) suggested that computing a high quality DTM in areas with very low penetration rate, i.e., where only a small percentage of pulses hit the bare ground surface, could be difficult. Actually, we found that the penetration rate of LiDAR pulses within hinoki cypress (*Chamaecyparis obtusa* Sieb. et Zucc.) plantations was very low as shown in Chapter 2. That is, because a DTM cannot always be generated easily and accurately in every forest stand, a procedure for estimating stand volume without generating and using the DTM created by mainly last pulse data should be developed. Such a procedure would free us from the troublesome post processing procedures that use last pulse data to generate an accurate DTM.

Therefore in this study, we propose a new single predictor variable for directly estimating stand volume without estimating and using the DTM and the tree height. The variable can easily be extracted using only first pulse data without generating and using a DTM. We also demonstrate the applicability of this variable by use of ground truth data of hinoki cypress plantations.

Materials and methods

Study area and ground truth data

The study area was the experimental forest of Tokyo University located in Aichi prefecture in central Japan (lat. 35°12' N, long.

Table 3-1. Summary of plot reference data at Site I (plot A-E; 72-year-old hinoki cypress stand) and Site II (plot F-H; 16-year-old hinoki cypress stand)

plot	plot area (m^2)	mean tree height (m)	mean stem diameter (cm)	stand volume (m^3/ha)
A	279	22.02	28.6	549.0
B	333	21.59	29.6	608.1
C	229	21.50	30.1	581.4
D	345	22.25	29.2	531.3
E	394	21.80	31.6	675.5
F	130	9.99	11.2	223.2
G	208	10.22	11.7	209.0
H	86	10.44	11.2	208.4

Table 3-2. The settings of the LiDAR system used in this study

Parameter	Performance
laser pulse frequency	20,000 H_z
scan frequency	24 H_z
scan angle	±30°
beam divergence	2.5 mrad
resolution	50 cm (flight speed 50 km/h, flight height 250 m)
3DGPS output information	yaw, roll, pitch, position, velocity, time
out put frequency of data	10 H_z
positioning method	differential method

Table 3-3. Accuracy of the LiDAR system used in this study

Parameter	Performance
self position of helicopter	±20 cm
posture of heicopter	3DGPS roll, pitch, yaw ±0.2°
measuring distance (maximum)	400 m
measuring distance (minimum)	50 m (for safe)
accuracy of measuring distance	±20 cm
accuracy of measuring angle	±1 mrad

137°10' E, 350 m a.s.l). Two pure hinoki cypress plantations, Site I and Site II, within compartment No.64 of this experimental forest were chosen for this study. The stand age of Site I and Site II were respectively 72-year-old and 16-year-old.

In Site I, fertilization and thinning had been carried out regularly from 1929 to 1979. There was several understorey vegetation. Five plots A, B, C, D, and E were established in this site. Site I faced the northwest and was mostly located on gentle slope; the one exception, plot E, was near a ridge and had a steeper slope than the other plots. Site II was a severe pruning experimental forest and the topography was flat. No evidence of fertilization or thinning was found. Three plots F, G and H were established at this site. The canopy density of plot F was very high, so there was few understorey vegetation in this plot. On the other hand, there was a few understorey vegetation in plots G and H because of the existence of some canopy gaps, which were nearly as large as an individual tree crown.

All tree positions (except dead or suppressed trees) within each plot were surveyed using a laser dendrometer (Ledha-Geo, Jenoptik laser, Jena, Germany) in the spring, 2001. For all trees within each plot, tree height was measured three times to the nearest centimetre and the mean value used for analysis. Diameter at breast height of all trees was also measured with a diameter tape to the nearest millimeter. A summary of plot reference data is listed in Table 3-1. The stand volume of each plot was calculated from the tree height and diameter at breast height of all trees using a standard two-way volume equation for hinoki cypress in Toyama, Gifu and Aichi districts (Forestry Agency 1970).

LiDAR data

The small-footprint LiDAR used in this study was a helicopter-borne laser scanner operated by Nakanihon Air Service Co., Ltd., Japan. The settings used are shown in Table 3-2 and accuracy of the LiDAR system is shown in Table 3-3. The LiDAR data used in this study were only first pulse data, which were acquired on 9th February 1999. The beam divergence of 2.5 mrad produced a footprint with a diameter of about 62.5 cm, and the average distance between footprints was approximately 69 cm along the scan line and approximately 59 cm along the flight line. After post processing, a Digital Surface Model (DSM) with a spatial resolution of 50 cm was generated from the first pulse data and subjected to further analysis.

Single predictor variable for stand volume and the procedures for calculating Vss

The pixels of a DSM generated from first pulse data would largely represent the sunny crown. As reported previously (Kajihara 1981a, 1981b, 1982), a close relationship has been found between crown dimensions and stem volume increment. Kajihara (1981a) indicated that the sunny crown mantle volume was the crown dimension variable most closely related with stem volume increment for hinoki cypress. We therefore analyzed the relationship between the sum of the sunny crown mantle volume estimated from LiDAR data (V_{ss} : m^3/ha) and the observed stand volume (V : m^3/ha). In this study, we then developed a procedure for calculating V_{ss} from a DSM using the following procedures.

Determination of the threshold for extracting vertical depth of the sunny crown mantle from DSM

Because the DSM would be largely composed of pixels representing pulses reflected by the sunny crown, we calculated V_{ss} from the vertical depth of the sunny crown mantle. To determine the sunny crown mantle depth, we first applied a minimum filtering to the DSM that the minimum pixel value within a window of N × N pixels was given to the central pixel (Jensen 1996). The raster data derived from the N × N minimum filtering was defined as DSM_{minN} (N: filtering window size).

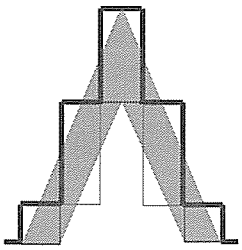

Fig 3-1. Example of calculating D_{ras} (sunny crown depth) using a 3 ×3 minimum filtering window. The thin solid line represents DSM_{min3} and the thick solid represents DSM. D_{ras} is the length of the rectangular areas formed from the thin and thick lines (i.e., D_{ras} = DSM − DSM_{min3}).

Assuming that the cross section of a coniferous tree crown is an isosceles triangle, and that the thickness of the crown mantle is constant, the raster data (D_{ras}) calculated by subtracting DSM_{minN} (thin solid line in Fig 3-1) from DSM (thick solid line in Fig 3-1) could then be regarded as the vertical depth of the sunny crown mantle. The cross sectional area of D_{ras} (rectangular areas formed from the thin and thick lines in Fig 3-1) could then be regarded as an approximation of the cross sectional area of the actual crown mantle (gray area in Fig 3-1).

In this study, three sizes of minimum filtering window were used (3 × 3 pixels, 5 × 5 pixels, 7 × 7 pixels) to change the vertical depth of the extracted sunny crown mantle in proportion to the filtering window size. Because the DSM could include pixels associated with canopy gaps, we used a histogram of the pixel values of D_{ras} to identify a threshold value (th_{sc}) for excluding such ground pixels.

Calculating the sunny crown mantle volume

For the D_{ras} calculated using each filtering window size, the sum of the sunny crown mantle volume within a plot was estimated as the sum of all pixel values (l_{sc} : m) less than th_{sc} (Σl_{sc}) multiplied by the area of each pixel (0.5 m × 0.5 m = 0.25 m^2). Then, V_{ss} was calculated as

$$V_{ssN}=\left(\frac{0.25\Sigma l_{sc}}{A}\right)\times 10000 \qquad (3\text{-}1)$$

where A (ha) is the plot area (Table 3-1) and N is the filtering window size. We investigated the relationships between V_{ssN} and observed stand volume (V) using regression analysis.

Results

Example histograms of D_{ras} data produced using 7 × 7 minimum filtering (Site I) and 3 × 3 minimum filtering (Site II) are shown in Fig 3-2. There were two remarkable peaks in all histograms. A definite second peak existed in all histograms of Site II as shown in Fig 3-2. The first peak primarily represented the vertical depth of the sunny crown mantle, while the second peak mainly represented the distance from the ground to the sunny crown

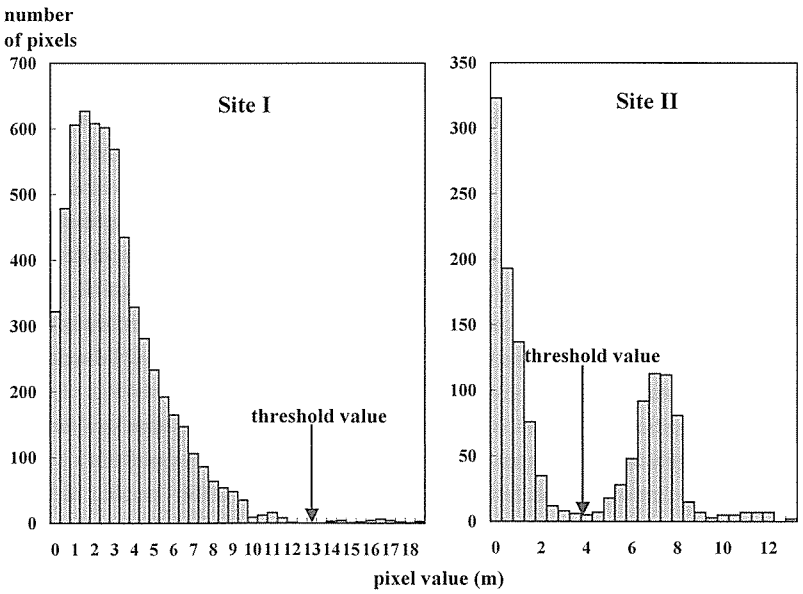

Fig 3-2. Sample histogram of the pixel value of D_{ras} (D_{ras}=DSM − DSM_{min3}) calculated for Site I (window size, N=7) and Site II (window size, N=3), respectively. The pixel values of D_{ras} are composed of both the vertical depth of sunny crown mantle and the distance from the ground to the sunny crown base. DSM_{minN} is raster data derived from N×N minimum filtering. The class interval is 0.5.

Table 3-4. Minimum filtering window size and threshold value (th_{sc}: m) used to discriminate pixel value associated with ground reflections. Regression equations (Eqs. a, b, and c) are the relationship between the sum of suuny crown mantle volume within a stand (V_{ssN} : m³/ha (N: filtering window window size)) and observed stand volume (V : m³/ha) for seven plots (Site I : plot A, B, C, D, and E in 72-year-old hinoki cypress stand, Site II : plot F,G, and H in 16-year-old hinoki cypress stand).

window size	threshold value (th_{sc})		regression equation	R^2 value
	Site I	Site II		
3 × 3	10.5	4	a: $V = 74.05 + 0.0327V_{ss3}$	0.952
5 × 5	13.5	3	b: $V = 155.75 + 0.0176V_{ss5}$	0.960
7 × 7	13.0	3	c: $V = 171.55 + 0.0136V_{ss7}$	0.958

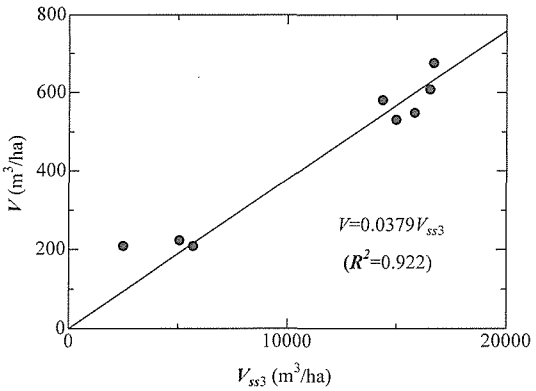

Fig 3-3. The relationship between variable associated with sum of sunny crown mantle volume within a stand (V_{ss3} : m³/ha) and observed stand volume (V : m³/ha)

base. Therefore, we used the mode method of thresholding (Suematsu and Yamada 2000), that is, the trough between the first and second peak was selected as the threshold (th_{sc}) and only pixel values less than th_{sc} were used for the calculation of V_{ssN} in Eq. 3-1. The value of th_{sc} identified for each minimum filtering window is shown in Table 3-4.

There was a close linear relationship between V and V_{ssN} for all three window sizes (Table 3-4). In addition, the intercept for the relationship between V and V_{ss3} did not differ significantly from zero. Finally, the relationship between V_{ss3} and V was expressed statistically as a simple ratio (Fig 3-3) as follows.

$$V=0.0379V_{ss3} \quad (R^2=0.922) \tag{3-2}$$

Discussion

Previous researchers have estimated stand volume using the LiDAR-derived tree height that calculated as the difference between DSM generated by first pulse data and DTM generated by last pulse data. However, forests with a low pulse penetration rate will not allow a DTM to be calculated easily or accurately (Kraus and Pfeifer 1998). Especially, in the hinoki cypress plantations, we found that the penetration rate of LiDAR pulses within was very low as shown in Chapter 2, and therefore LiDAR pulse penetration of the forest canopy is also considered to be too low to enable a reliable DTM to be calculated. Then, if a DTM cannot be generated, tree height, and thus stand volume, cannot be estimated with the method presented by the previous researchers (e.g., Kraus and Pfeifer 1998; Axelsson 1999; Elmqvist 2000; Brovelli *et al.* 2004). On the other hand, the procedure presented in this study used only the DSM that can be easily generated using first pulse data, and therefore did not require the calculation of a DTM.

Some researchers (e.g., Maclean and Krabill 1986; Nelson 1988) have also reported the procedures for estimating stand volume using a measure of the canopy profile cross-sectional area generated by laser profiling data without generating and using a DTM. However, as suggested by Næsset (1997a), the laser profiling technique, which records a single line of data directly beneath the aircraft, would provide a rather more limited sample than the scanning laser systems used in this study. In particular, in forest where canopy gaps or non-forested areas are irregularly distributed, the location of the trace of the laser profiling could have a considerable influence on the volume estimation. On the other hand, in our procedure the influence of canopy gaps or non-forested areas can be excluded prior to volume estimation. Although we used the mode method to discriminate the pixels of the sunny crown from those of the ground or non-sunny crown in this study, th_{sc} could also be estimated automatically using statistical thresholding, e.g., Otsu's method (Otsu 1979) or Niblack's method (Niblack 1986). We could then automatically calculate V_{ssN} from DSM, because th_{sc} was the only value determined manually in the procedure presented in this study.

Although there was a small time lag between the acquisition of the LiDAR data and the ground truth data, the ratios between the stem volumes within a stand would not change much between the two acquisition times. Therefore, the strong linear relationships between V and V_{ssN} shown in Table 3-4 could be considered to be the same as if V had been surveyed at the same time that the LiDAR data were acquired. In addition, comparing our results with those of previous experiments that succeeded in estimating stand volume using an accurate DTM (Hyyppä and Inkinen 1999; Means *et al.* 2000), the R^2 value of Eq. 3-2 presented in this study was higher than or nearly equal to those of the previous studies. Certainly V_{ss3} would be easier to calculate than predictor variables such LiDAR-derived tree height calculated using a DTM. Therefore, if we want to obtain estimates of stand volume easily,

quickly and accurately, the procedure presented in this study would offer a viable alternative to methods that rely on a DTM generated from last pulse data (e.g., Maltamo *et al.* 2004; Means *et al.* 2000; Persson *et al.* 2002). In addition, combining the DTM-based methods with the method presented in this study offers the possibility of reducing unexplained variation, and thus, even more accurately estimating stand volume, especially for coniferous forests.

The results of this study indicated that a single predictor variable (V_{ssN}) associated with the sum of the sunny crown mantle volume within a stand was highly correlated with observed stand volume (V) in hinoki cypress plantations. In particular, the relationship between V_{ssN} and V was expressed as a simple ratio when a 3 × 3 minimum filtering window was used. Thus, V_{ssN} is considered to be a useful single predictor variable for estimating stand volume in hinoki cypress plantations; it is also very simple and convenient to calculate. Further work is needed to verify the broader applicability of the regression equations presented in this study to other stands of hinoki cypress and to investigate whether the method is just as applicable to other coniferous forests.

Chapter 4. Forest measurement in sugi (*Cryptomeria japonica* D. Don) plantations by small-footprint airborne LiDAR

(4a) Individual tree height estimation

Introduction

Some useful studies have demonstrated that recent commercial small-footprint airborne LiDAR systems, as listed in Baltsavias (1999b), could measure individual tree height and estimate stem volume accurately in boreal coniferous forests (Hyyppä and Inkinen 1999; Hyyppä *et al.* 2001; Persson *et al.* 2002). In Japan, Yone *et al.* (2002) and Omasa *et al.* (2003) showed that small-footprint airborne LiDAR was capable of precisely measuring and estimating individual tree characteristics in Japanese larch (*Larix leptolepis*) and sugi (*Cryptomeria japonica* D. Don) plantations, respectively.

However, for the application of small-footprint airborne LiDAR to forest monitoring, especially with regard to tree height estimation, most previous studies appeared to have succeed in estimating individual tree height accurately only in flat terrain (e.g., Hyyppä and Inkinen 1999; Hyyppä *et al.* 2001; Persson *et al.* 2002; Yone *et al.* 2002; Omasa *et al.* 2003). Principally, tree height estimates using small-footprint airborne LiDAR data should be calculated by subtracting the estimated ground elevation value from the elevation value of the outer vegetation layer of a canopy. Thereby, the accuracy of the estimated ground elevation would affect tree height estimates. Kraus and Pfeifer (1998) showed that in Vienna Woods, the larger the slope angle, the lower is the accuracy of LiDAR-estimated ground height. Therefore, there is no account of whether tree height could be estimated accurately in mountainous forest, the topography of which is likely to be steeper and more complex than that of previously researched sites. Though Heurich *et al.* (2003) mentioned that LiDAR-derived tree height estimates must be corrected when the slopes are steeper than 20°, they did not investigate the accuracy of LiDAR-derived tree height estimates for different slope angles in detail. Mountainous forests in Japan have usually steeper (well over 20°) and more complex topographies; hence a more detailed research is required with regard to tree height estimation with small-footprint airborne LiDAR in such mountainous areas.

Since we have already found in Chapter 2 that the penetration rate of LiDAR pulses that hit the ground in sugi stand was much higher than that of hinoki cypress stand, and would have a possibility to create DTM enough to estimate individual tree height using the methodologies presented by some previous researchers (e.g., Kraus and Pfeifer 1998; Axelsson 1999; Elmqvist 2000; Holmgren *et al.* 2003a; Brovelli *et al.* 2004). We therefore investigated the accuracy of LiDAR-derived individual tree height estimates for different types of topographical features of even-aged sugi plantations located in a mountainous area. Prior to estimating individual tree height, we first investigated the number of detected trees within plots by identifying LiDAR-detected trees as corresponding field trees. Next, the average error between LiDAR-derived tree heights and field measured tree heights was computed to investigate the influences of topographical features on systematical differences, i.e., either underestimates or overestimates. Subsequently, root mean square errors between these values were investigated to evaluate the accuracy of the estimates.

Materials and methods

Ground reference data

The study area was the Nagoya University experimental forest located in the Aichi Prefecture in central Japan (lat. 35° 12' N, long. 137° 33' E, 930 m asl). Even-aged sugi plantations that had not been properly managed were chosen for this study because they are representative of several such sugi plantations in Japan. One square plot (plot 1: approximately 50 × 50 m) consisted of a location, the terrain of which had a gentle to steep slope (Fig 4a-1). Plot 1 mainly consisted of planted sugi (233 trees); however, planted hinoki cypress (21 trees), akamatsu (*Pinus densiflora*) (2 trees), urajiromomi (*Abies homolepis*) (2 trees), and sawara (*Chamaecyparis pisifera*) (2 trees) were also mixed in. The forest floor was covered with litter, and the understorey vegetation that had not been weeded mainly consisted of kumazasa (*Sasa veitchii*) and shiromoji (*Lindera triloba*) with a height that was less than approximately 2 m. The other square plot (plot 2: approximately 25 × 25 m) consisted of a gentle slope with a slightly rough surface. Only sugi (50 trees) existed in plot 2 (Fig 4a-1), and the

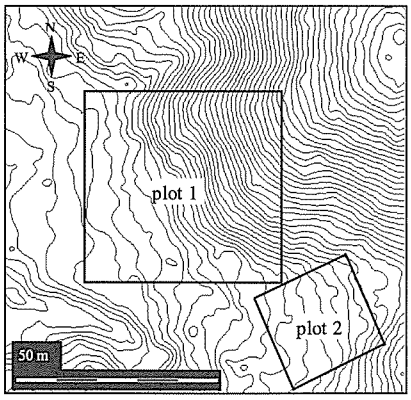

Fig 4a-1. Location of plot 1 (2500 m^2) and 2 (625 m^2) on the topographic map of this study area. The contour is generated using a digital terrain model created with LiDAR data and the interval is 1 m.

Table 4a-1. Increments of tree height and stem diameter between 2001 and 2003 for three sample sugi (*Cryptomeria japonica* D. Don) trees.

	Stem1	Stem2	Stem3	Average
Tree height increment	1.029	1.012	1.027	1.023
Stem diameter increment	1.028	1.027	1.022	1.026

Table 4a-2. Summary of plot reference data (sugi (*Cryptomeria japonica* D. Don) trees) used for analysis

Characteristic	Range	Mean ± S.D.[d]	Stand level
Steep slope (184 trees)			
Slope angle (degree)[a]	25.0–47.8	37.6 ± 5.8	
Tree height (m)	8.7–28.9	18.9 ± 2.9	
DBH (cm)[b]	9.8–43.4	24.8 ± 6.4	
Crown radius (m)	0.4–2.7	1.5 ± 0.4	
Stem volume (m^3)[c]	0.05–1.83	0.49 ± 0.28	
Stand density (trees/ha)			1227
Stand volume (m^3/ha)			504.8
Gentle slope (50 trees)			
Slope angle (degree)[a]	11.4–21.0	15.6 ± 3.7	
Tree height (m)	11.9–25.2	20.4 ± 2.9	
DBH (cm)[b]	17.7–47.8	30.7 ± 6.7	
Crown radius (m)	1.1–3.4	1.9 ± 0.4	
Stem volume (m^3)[c]	0.15–1.85	0.75 ± 0.37	
Stand density (trees/ha)			714
Stand volume (m^3/ha)			499.6
Gentle yet rough terrain (50 trees)			
Slope angle (degree)[a]	3.3–29.7	16.8 ± 7.8	
Tree height (m)	13.5–27.6	22.3 ± 3.1	
DBH (cm)[b]	15.9–40.6	30.4 ± 6.8	
Crown radius (m)	0.7–2.5	1.5 ± 0.4	
Stem volume (m^3)[c]	0.14–1.56	0.81 ± 0.37	
Stand density (trees/ha)			800
Stand volume (m^3/ha)			602.9

[a]Slope angle was computed by a digital terrain model created from LiDAR data.

[b]DBH denotes diameter at breast height

[c]Stem volume was calculated by using a standard two-way (tree height and diameter at breast height) volume equation.

[d]S.D. denotes standard deviation.

understorey vegetation (also unweeded and height less than approximately 2 m) mainly consisted of shiromoji; some big stones and litter also existed on this forest floor.

As mentioned above, the terrain of plot 1 consisted of steep and gentle slopes. To investigate the effect of the different topographical features on LiDAR-derived tree height, slope angles within the plots were first computed by a digital elevation model that had been created using LiDAR data. Next, a regular grid-covering plot 1 was generated on a computer using GIS. The size of the individual grid cells was approximately 10 × 10 m. The topographical features in plot 1 were then divided into two categories. An area composed of fifteen grid cells (i.e., approximately 1500 m^2), with a mean slope angle of approximately 38°, was defined as "steep slope." Another area composed of seven grid cells (i.e., approximately 700 m^2), with a mean slope angle of approximately 16° was defined as "gentle slope." The remaining three grid cells in plot 1 (i.e., approximately 300 m^2) were excluded form this study because only one sugi tree and many hinoki cypress trees (approximately 76%) existed in these three grid cells. Contrarily, though the terrain surface in plot 2 was rougher than the "gentle slope" area in plot 1, the mean slope angle was approximately 17°. Therefore, the entire area of plot 2 (i.e., approximately 625 m^2) was defined as "gentle yet rough terrain," which was the third topographical category assessed.

During fall and winter of 2003 and 2004, i.e., after the growth season had ended, tree measurements were completed. Static GPS surveys were used to determine the accurate position of a reference point in an open area near the plots; subsequently, the tree positions were surveyed in relation to the reference point as follows. The position of the center of all tree stems (except dead trees) within the two plots was measured using a compass with an accuracy of 1° and a portable laser distance measurement with an accuracy of 1 mm (DISTO4, Leica Geosystems, Heerbrugg, Switzerland), thus making corrections for the stem diameter at height at which the laser beam is incident. Additionally, the heights of the trees and their diameters at breast height (1.3 m above ground level) were measured using a dendrometer with an accuracy of 1 cm (Ledha-Geo, Jenoptik laser, Jena, Germany) and a diameter tape, respectively. Subsequently, the projected on-ground crown radii at a height of 1.3 m above ground level (eight directions) were measured accurately.

There was approximately a two-year gap between the acquisition time of the LiDAR data (summer 2001) and the ground truth data (fall and winter 2003). To ascertain the two-year increment in tree height and stem diameter, stem analysis was performed on three sample sugi trees that had been growing near plot 2 (Table 4a-1). The age of the stands in this study area, including these three trees, was 48 years. The arithmetic mean value of the increment for the trees was then deducted from the ground truth data in plots 1 and 2. The corrected data was defined as field data and subsequently used for analysis in this study. However, the crown radius was not corrected; in the analysis in this study, detecting tree tops and estimating tree height were performed only for sugi trees. A summary of the plot reference data (only for sugi) is listed in Table 4a-2.

LiDAR data collection

The laser data acquisition was performed on August 17, 2001 using a helicopter-borne laser scanner operated by Nakanihon Air Service Co., Ltd., Japan. The pulsed laser beam moves across the helicopter track controlled by a scanner and along through the forward motion of the helicopter. The resulting pattern on the ground is thus Z-shaped. In this study, the position of the reflecting object was determined from the first and second pulse, respectively. Laser measurements were made on a single flight line. The beam divergence was 0.5 mrad, giving a footprint diameter of approximately 0.15 m. The flight altitude above ground level was approximately 300 m and its speed was 43 km/h. The scan mirror frequency, laser pulse frequency, and the scan width were 24 Hz, 20 000 Hz, and ±30°, respectively. By this setting, the average distance between footprints was approximately 0.42 m along the scan line and approximately 0.5 m along the flight line. The elevation depth accuracy of the distance measured by the LiDAR system used in this study was approximately 0.1-0.25 m at a flying altitude of 200 m.

Processing LiDAR data and creating a Digital Surface Model (DSM), Digital Terrain Model (DTM), and Canopy Height Model (CHM)

No parameter settings were changed during the processing of the LiDAR data for all topographical features in the study area. The laser sampling density was theoretically 4.76 points/m^2 with the LiDAR settings used in this study; however, the actual laser sampling density was greater than the theoretical value; 8.80 points/m^2 (steep slope), 15.60 points/m^2 (gentle slope), and 11.55 points/m^2 (gentle yet rough terrain). Therefore, the unevenly distributed laser reflection point data was converted into two raster layers with a pixel size of 1/3 m. The first raster layer, referred to as DSM_{raw}, was assigned the height value of the highest laser reflection point within each pixel using only first pulse data. The second raster layer, referred to as DTM_{raw}, was assigned the lowest laser reflection point within each pixel using both first and second data.

To create a continuous surface model, that is, a Digital Surface Model (DSM), the value of the no-data pixels in DSM_{raw} was interpolated by an inverse distance weighting (IDW) method that did not change the original value. IDW is a weighted average interpolator method; the weight given to a particular data point when calculating a grid node is proportional to the inverse of the distance of the observation from the grid node (Popescu *et al.*

2002). The interpolated DSM_{raw} was defined as DSM.

In this study, DTM_{raw} contained several unexplained noise pixels, the values of which were distinctly below ground level, as mentioned by Holmgren *et al.* (2003a), along with other unexplained noise pixels, the values of which were higher than those of the DSM. Such noise pixels within DTM_{raw} were removed, and the method used by Holmgren *et al.* (2003a) was then applied to acquire a Digital Terrain Model (DTM) as follows. Each center pixel was compared with other pixels within a 4 m horizontal distance, and if the vertical angle of the neighboring pixels from the center pixel exceeded 50°, the center pixel was classified as ground and the neighboring pixels were removed. Subsequently, those pixels that remained were also referred to as ground. Finally, a continuous terrain surface model, i.e., DTM was created by spline interpolation using the pixels that remained (Magnussen and Boudewyn 1998; Magnussen *et al.* 1999; Riaño *et al.* 2003).

To estimate individual tree height, first, a Canopy Height Model (CHM) was computed by subtracting DTM from DSM. CHM can be used to represent a canopy height raster layer in wooded areas. In the open areas and gaps between the trees, this height will be close to zero; thus, representing ground laser hits (Næsset 2002). Observations with a height value less than 2 m were excluded to eliminate ground hits and the effect of stones, shrubs, etc. from CHM (Næsset 1997a, 1997b, 2002; Persson *et al.* 2002).

Detecting individual tree tops

Individual tree tops were detected by local maximum filtering, a common technique used to identify tree locations on high-resolution optical images (Wulder *et al.* 2000). Local maximum filtering is used for optical images based on the fact that the reflectance of a tree crown is typically greatest at its apex. This operates on the assumption that for LiDAR data the highest laser elevation value among laser hits of the same tree crown is the apex (Popescu *et al.* 2002), and the method has been used in many previous studies for identifying tree locations using small-footprint airborne LiDAR data (e.g., Holmgren *et al.* 2003a; Hyyppä *et al.* 2001; Maltamo *et al.* 2004; McCombs *et al.* 2003; Popescu *et al.* 2002, 2003; Zimble *et al.* 2003). That is, if the central pixel has the elevation value which is greater than any other pixel value within a window, the central pixel is regarded as tree top. In this study, the selected moving window size was 3×3 pixels (Hyyppä *et al.* 2001, Maltamo *et al.* 2004). To delete the noise in individual tree crowns of CHM before detecting tree tops in order to make it more likely that each tree has a single height maxima, a simple convolution Gaussian filter was used for CHM (Hyyppä *et al.* 2001; Suematsu and Yamada 2000). Subsequently, local maximum filtering was performed for the smoothed CHM.

Processing field crown data

GIS produced octagonal crown projections (vector data) with the eight directional field measured crown radii. Subsequently, each crown segment (raster data) with a pixel size of 1/3 m was created by converting the vector data to raster data. Since the viewing of suppressed or intermediate tree crowns by aerial surveillance in an actual stand is often difficult, the overlap between crown segments was assigned to relatively tall trees in GIS.

Evaluation method for detected tree tops and estimates of tree heights

Before evaluating the accuracy of the estimates of individual tree height, each detected tree top (LiDAR-detected tree top) had to be identified as the corresponding field stem position within the crown segment in a two dimensional plane. If one LiDAR-detected tree top existed within a segment, the detection was correct. If several LiDAR-detected tree tops existed within a segment, the field stem position was identified as the pixel with the highest values, and the remaining unidentified pixels were defined as commission errors. If any LiDAR-detected tree tops existed beyond crown segments within a plot, this was also defined as a commission error. However, if no LiDAR-detected tree top existed within a segment, this error was defined as an omission error. Subsequently, tree heights of the detected trees (LiDAR-derived tree height) were computed as the maximum value of unsmoothed CHM within the crown segments (Maltamo *et al.* 2004).

The relationships between the LiDAR-derived tree height and the field tree height for the detected trees for each topographical feature were investigated by regression analysis, in which lines were fitted to the data using the least-squares method. The mean difference, i.e., the average error ($\bar{D}$) between the LiDAR-derived tree height h_L (m) and the field measured tree height h_f (m) was then evaluated to investigate the influences of topographical features on the systematical differences, i.e., either under-estimates or overestimates. The statistical significance of the average error was assessed by means of two-tailed t-tests (Næsset 1997a). The average error (m) was computed using the following equation:

$$\bar{D} = \frac{1}{n}\sum_{i=1}^{n}(h_{L(i)} - h_{f(i)}) \tag{4a-1}$$

where h_L and h_f are LiDAR-derived tree heights and the field tree heights, respectively, for the detected trees. The number of detected trees is n and i was the detected tree number. Subsequently, to evaluate the accuracy of the LiDAR-derived tree height estimates, Root Mean Square Error (RMSE) (m) was also computed as follows:

$$\mathrm{RMSE} = \sqrt{\frac{\sum_{i=1}^{n}\left(h_{L(i)} - h_{f(i)}\right)^2}{n}} \tag{4a-2}$$

where h_L, h_f, n, and i were the same as in Eq. 4a-1. To evaluate the

effect of DTM for estimating tree height, the accuracy of the DTM created in this study was also examined by Eq. 4a-1 and 4a-2. However, in the examination of the accuracy of the DTM, h_L, h_i, n, and i represented the elevation values of DTM, field-measured ground elevation for all the tree stems, number of all field-measured trees, and all field measured tree numbers, respectively, within plots consisting of not only sugi but also hinoki cypress, akamatsu, sawara, and urajiromomi.

However, according to previous reports, laser sampling density could affect the counting of stem numbers (Yone *et al.* 2002) and estimates of tree heights (Næsset and Økland 2002). Since most previous studies, as well as the present one, have detected tree tops and estimated individual tree heights using raster LiDAR data, laser sampling density could be expressed by using the number of pixels of first pulse raster data in DSM_{raw} within crown segments in this study. Thus, to discuss the effect of laser sampling density on both the number of detected trees and the accuracy of the estimates of tree height, the percentage of the number of pixels with non-null values in DSM_{raw} within all tree crown segments was computed for each topographical feature.

Results

The percentage of laser pulses hitting crowns and the number of detected trees

The percentage of the number of pixels of first pulse raster data in DSM_{raw} within crown segments was the highest in the gentle yet rough terrain (67.2%) and the lowest in the gentle slope (50.2%) (Table 4a-3). In all topographies, commission errors were lower than omission errors. Omission errors in the steep slope were the highest among all the topographical features; 74% of the trees were correctly detected (Table 4a-4). On the other hand, in the other topographies, particularly in the gentle yet rough terrain, most trees were correctly detected (Table 4a-4). Otherwise, the tree heights and crown radii of undetected trees were usually less than those of the mean value in each topographical feature (Fig 4a-2).

Estimates of individual tree height and ground elevation

The coefficients of determination (R^2) of the regression equations for LiDAR-derived and field tree heights for the three topographical features (steep slope, gentle slope, and gentle yet rough terrain) were 0.857, 0.923, and 0.955, respectively (Fig 4a-3). The intercepts of all regression equations in Fig 4a-3 did not significantly differ from zero ($p > 0.05$), indicating that the average error of the regression equations was not significant. The slopes for all regression equations could be statistically regarded as one ($p < 0.01$), indicating that the LiDAR-derived tree height was independent of different tree heights.

The average error of the LiDAR-derived tree height was highest in the gentle slope and lowest in the gentle yet rough

Table 4a-3. Percentage of the numberof pixels of first pulse raster data in DSM_{raw} within crown segments

Topography	Percentage (%)
Steep slope	58.9
Gentle slope	50.2
Gentle yet rough terrain	67.2

The percentage is calculated by the number of pixels with non-null values in DSM_{raw} within all tree crown segments. DSM_{raw} is a raster layer that is assigned the height value of the highest laser reflection point within each pixel using only first pulse data.

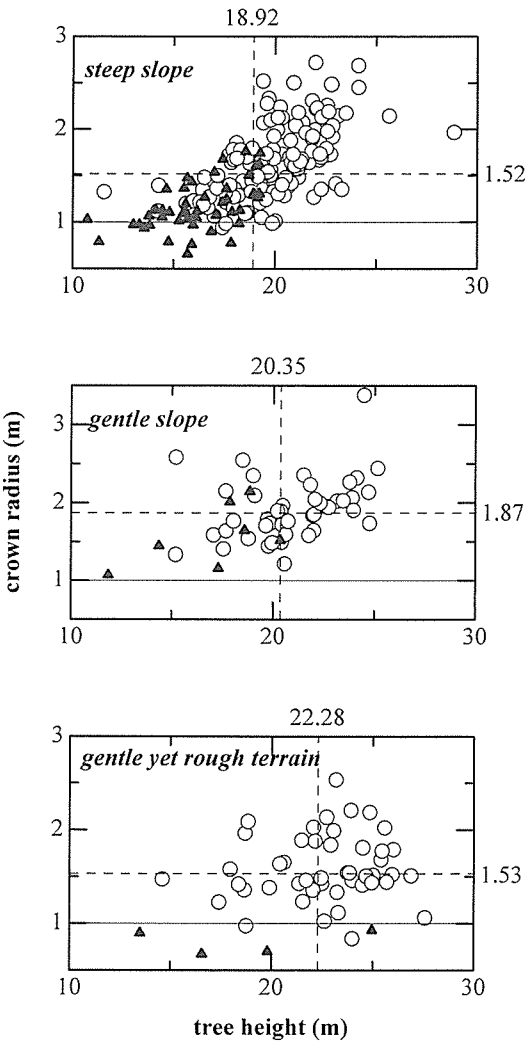

Fig 4a-2. Characteristics of detected and undetected trees based on the relationship between tree height and crown radius. White circles and black triangles denote detected and undetected trees, respectively. Vertical and horizontal dashed lines denote the mean value of tree height and crown radius, respectively.

Table 4a-4. Number of detected trees

Topography	Number of detected trees			Actual number
	Correct	Commission[a]	Omission[b]	of trees
Steep slope	136 (74%)	6 (3%)	48 (26%)	184
Gentle slope	43 (86%)	5 (10%)	7 (14%)	50
Gentle yet rough terrain	46 (92%)	1 (2%)	4 (8%)	50

[a]Commission denotes that if several LiDAR-detected tree tops existed within a crown segment, the field stem was identified as the pixel with the highest values, and the remaining unidentified pixels were defined as commission errors. If any LiDAR-detected tree top existed out of the crown segments within a plot, this was also defined as a commission error.

[b]Omission denotes that if no LiDAR-detected tree top existed within a crown segment, this error was defined as omission error.

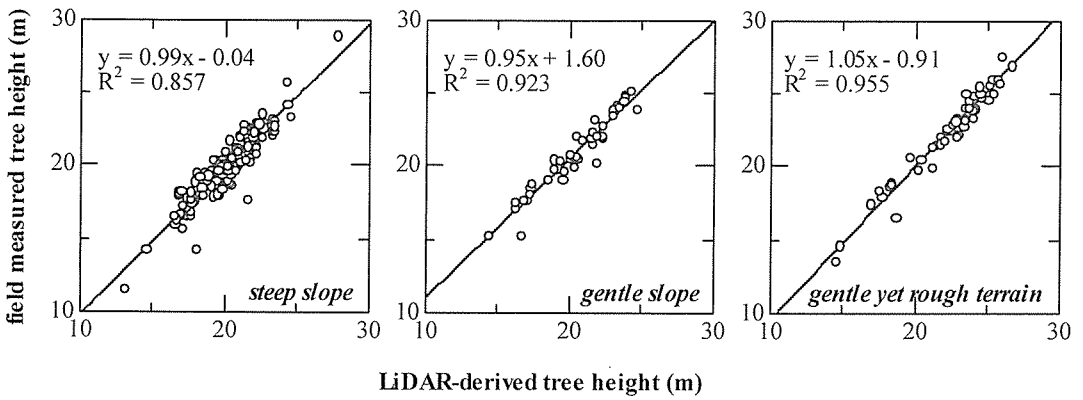

Fig 4a-3. The relationship between LiDAR-derived and field-measured tree heights.

Table 4a-5. Average error and RMSE between field measured and LiDAR-derived data

Topography	Ground elevation (m)		Tree height (m)	
	Average error[a]	RMSE[b]	Average error[a]	RMSE[b]
Steep slope	-0.199**	0.577	0.227**	0.901
Gentle slope	0.106*	0.316	-0.473**	0.846
Gentle yet rough terrain	0.101**	0.267	-0.183*	0.576

* $P < 0.05$; ** $P < 0.01$

[a]Average error was computed using Eq.4a-1 in the text.

[b]RMSE denotes root mean square error and was computed using Eq.4a-2 in the text.

terrain (Table 4a-5). However, the highest RMSEs of tree height and ground elevation estimates were in the steep slope. The average error of ground elevation estimates was also the highest for the steep slope.

Discussion

The main objectives of this study were the investigation of the number of detected trees and the accuracy of individual tree height estimates of sugi plantations in a mountainous area for three types of topographical features. An accurate field survey of all stem positions and the projected on-ground crown radii within plots, enabled the accurate identification of LiDAR-detected tree tops as the corresponding field stem positions within the crown segments in a two dimensional plane. This correct identification enabled the evaluation of the estimates of LiDAR-derived individual tree heights.

Fig 4a-2 shows the characteristics of detected and undetected trees, taking note of the relationship between tree height and crown radius, in each topographical feature. Magnussen *et al.* (1999) asserted that in their experience, six to ten laser hits per tree crown would be needed to clearly distinguish between individual tree crowns. That is, assuming that the tree crown was circular in shape and that the crown radius was 1 m, at least two or three hits per square meter would be needed. Though the settings of the LiDAR system used in this study would theoretically produce approximately four laser hits per square

meter, the results of this study showed that trees with a crown radius of less than 1 m (thin solid lines denote a 1 m crown radii in Fig 4a-2) were hardly detected in each topographical feature in this study. Therefore, a greater laser sampling density might be needed to detect such small trees with a crown radii less than 1 m. It is difficult to detect trees with a size smaller than the mean size (an intersection of vertical and horizontal dashed lines in Fig 4a-2); however, most canopy trees with sizes larger than the mean size could be accurately detected in every topographical feature.

Though 49.8% (i.e., 100 - 50.2 %) pixels in DSM_{raw} within crown segments were interpolated in the gentle slope (Table 4a-3), 86% of the trees were accurately detected from DSM in the gentle slope (Table 4a-4). Considering that correct interpolation for DSM_{raw} was needed to detect individual tree tops from DSM, this result indicates that fine interpolation that was at least convenient for local maximum filtering had been performed by IDW interpolation for DSM_{raw} and a Gaussian smoothing for CHM in this study. This would be applicable to other topographical features. To identify individual tree crowns from LiDAR data, some previous researchers have applied a watershed method for detecting tree crowns (e.g., Yone *et al.* 2002). While it is unknown as to which method would be superior; the local maximum filtering method can be considered to be a good method for detecting individual canopy tree tops in sugi plantations in mountainous areas.

The average errors between LiDAR-derived and field measured tree heights in both the gentle slope and the gentle yet rough terrain were negative values (Table 4a-5). Even if the influences of the positive average error of DTM were deducted, the average error of the LiDAR-derived tree height was still negative, i.e., underestimates of tree height. Moreover, underestimates of tree height in the gentle slope were greater than those in the gentle yet rough terrain. Persson *et al.* (2002) explained that low laser sampling density caused tree height underestimation in their study; thus indicating that because the uppermost parts of the tree tops were not likely to be hit when using small-footprint airborne LiDAR, the estimates of tree heights would consequently be underestimates. According to Gaveau and Hill (2003), the failure to sample tree tops because of an insufficient laser sampling density is likely to be of greater relevance in coniferous woodlands where crown shape is more conical than in broadleaf woodlands where crowns are more rounded. Næsset and Økland (2002) concluded that the observed standard deviations in tree height residuals in LiDAR data for a forest dominated by Norway spruce (*Picea abies*) could be improved by increasing sampling density. Considering these reports, the greater underestimates of tree heights of sugi in the gentle slope than those in the gentle yet rough terrain in this study were considered to be caused by the lower percentage of first pulse data in DSM_{raw} within crown segments in the gentle slope (Table 4a-3). Though a significant difference between field measured and LiDAR-derived heights exists, as shown in Table 4a-5, even the highest negative average error in the gentle slope was only -0.478 m.

The average error of the LiDAR-derived tree height in the steep slope was conversely a positive value (Table 4a-5). Even if the influence of the negative average error of DTM was deducted, the average error of the LiDAR-derived tree height was still positive, i.e., an overestimate of tree height. The cause was considered to be the horizontal positional error between the tree top and stem (Heurich *et al.* 2003). This is because even coniferous tree stems are not always upright in an actual forest stand and the tops are likely to be tilted to the valley side. Particularly on a steep slope, the LiDAR-derived tree height calculated with the distance between the tree top and just below ground surface would be an overestimate (Hirata 2004). More detailed research about the overestimation of tree heights on steep slopes is needed. However, though a significant difference between field measured and LiDAR-derived heights on steep slopes exists, the positive average error was only 0.227 m.

The RMSE in every topographical feature was less than 1 m (Table 4a-5), but the RMSE of LiDAR-derived tree height was greater than that of the LiDAR-derived ground elevation in each of the topographical features. The cause could be attributed to the fact that there was a lag of approximately two years between the time when the LiDAR data (2001 year) was acquired and the time when the ground truth data (2003 year) was obtained. Though the arithmetic mean value of the increment for the trees was uniformly deducted from the ground truth data in this study, in an actual stand, the increments of the tree parameters, e.g., height, stem diameter, crown diameter, and volume differ for each tree. Therefore, because the true height of trees in 2001 might not have been accurately estimated by deducting a uniform increment, the accuracy of the LiDAR-derived tree height estimates would be lower than the LiDAR-derived ground elevation estimates. However, the maximum value of the errors in the LiDAR-derived tree height estimates in every topographical feature was 1 m.

In this study, though significant average errors with positive or negative values for LiDAR-derived tree heights existed in every topographical feature, the accuracy of the LiDAR-derived tree height estimates (RMSE) was in fact less than 1 m in the sugi plantations included in this study. Moreover, though no parameter settings were changed during processing of the LiDAR data for all the topographical features investigated in this study area, the accuracy of the tree height estimates was still high for every topographical feature. Therefore, the results of this study indicated that small-footprint airborne LiDAR will be a useful tool for accurately estimating individual canopy tree heights in even-aged sugi plantations in mountainous areas.

(4b) Estimation of individual stem volume and stand volume

Introduction

The data acquired from recent commercial small-footprint airborne LiDAR systems, as listed in Baltsavias (1999b), may possibly offer three-dimensional information regarding individual trees, such as tree height, crown area or diameter, and stem volume, whereas large-footprint LiDAR will contain information on the forest canopy and multiple forest elements rather than individual trees (Lim *et al.* 2003). In particular, with regard to tree height estimation, previous researchers showed that individual tree height was accurately estimated in boreal coniferous forests with a flat terrain (Hyyppä and Inkinen 1999; Hyyppä *et al.* 2001; Maltamo *et al.* 2004; Persson *et al.* 2002) and also in Japanese larch (*Larix leptolepis*) (Yone *et al.* 2002) and sugi (*Cryptomeria japonica* D. Don) plantations (Omasa *et al.* 2003) with a flat terrain in Japan. In Chapter 4a, we showed that the accuracy of the LiDAR-derived tree height estimates by root mean square error was less than 1 m in even-aged sugi plantations located in a mountainous forest in Japan; the topography of this region is probably steeper and more complex than that of previously researched sites. Furthermore, previously, most researchers estimated the individual stem volume directly or indirectly using LiDAR-derived estimates. A few researchers (Hyyppä and Inkinen 1999; Hyyppä *et al.* 2001; Maltamo *et al.* 2004; Persson *et al.* 2002) indirectly estimated the stem volume using a standard two-way volume equation with the LiDAR-derived tree height and stem diameter at breast height (DBH) calculated from the LiDAR-derived tree height and crown area (or diameter). These researchers used the regression equation of field-measured DBH against field-measured tree height and crown diameter. On the other hand, Holmgren *et al.* (2003a) directly estimated the stem volumes using the regression equation of the field-measured stem volume against the LiDAR-derived tree height together with the LiDAR-derived crown area. This method would be more useful because the stem volumes can be directly predicted with variables derived from the LiDAR data without estimating the DBH. With regard to this method, apart from the crown area, there may be other useful predictor variables with respect to the crown properties for individual stem volume prediction. In Chapter 3, we experimentally determined that there was a close linear relationship between the stand volume and the LiDAR-estimated sum of the sunny crown mantle volume within a plot in hinoki cypress (*Chamaecyparis obtusa* Sieb. et Zucc.) plantations. Therefore, it is important to investigate which LiDAR-derived crown properties together with the LiDAR-derived tree height estimates can be useful in regression models to predict individual stem volumes.

Stand characteristics, e.g., stem density and statistics of tree height, DBH, crown radius, and stem volume, differed among the stands with different topographical features in even-aged sugi plantations located in a mountainous forest. In Chapter 4a, in the analysis of LiDAR data, these differences did not affect the estimation of individual tree height; however, they affected the detection of individual trees. Since we generally calculate the stand volume by summing the individual stem volumes, the differences could potentially affect the estimation of stand volume using the LiDAR data.

Therefore, in this study, we first investigated which predictor variables with respect to crown properties, derived from small-footprint airborne LiDAR data, could be useful in the regression model to predict individual stem volumes within stands that has different stand characteristics with different topographical features in mountainous forests. Moreover, we compared sum of field-measured stem volumes with sum of LiDAR-derived stem volume estimates predicted by the best regression model for LiDAR-detected trees. Subsequently, the sum of predicted stem volumes for detected trees were compared with actual stand volume, i.e., the field-measured total stem volumes for all trees within each stand.

Materials and methods

Ground reference data and LiDAR data

The study area and the ground reference data are the same as those reported in Chapter 4a, so please see 'Materials and methods' in Chapter 4a. A summary of the plot reference data is listed in Table 4a-2 in Chapter 4a. The individual stem volumes were calculated from the corrected tree height and the DBH in Chapter 4a using a standard two-way volume equation for sugi in Toyama, Gifu, and Aichi districts (Forestry Agency 1970). Moreover, the settings of the LiDAR system are also the same as those reported in Chapter 4a.

Preprocessing LiDAR data and creating a digital surface model, digital terrain model, and canopy height model

The methods for preprocessing LiDAR data and creating a digital surface model (DSM), digital terrain model (DTM), and canopy height model (CHM) were the same as those reported in Chapter 4a.

Segmentation of individual tree crowns

Individual tree crowns were identified using our software named LiDAS (LiDAR Data Analysis System), which has the ability to identify individual canopy gaps, segment tree crowns, etc. In order to locate trees, the low-pass filtered (i.e., smoothed) DSM was searched for local maxima, the positions of which were considered to be tree tops and seed points for crown segmentation, and subsequently, for seeded region growing segmentation. This system requires the determination of an important threshold value, which is the difference between the height of the crown base within the smoothed DSM and the ground surface height of

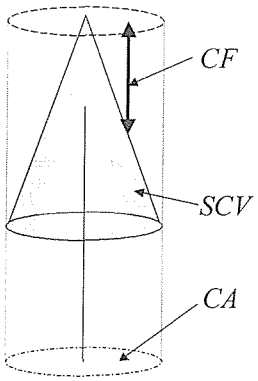

Fig 4b-1. A simple model of single tree and LiDAR-derived crown properties are shown. *CA* (m^2) denotes LiDAR-measured crown area, i.e., crown projection area. *SCV* (m^3) and *CF* (m) denote LiDAR-estimated sunny crown mantle volume (gray area in the figure) and crown form were computed using Eqs. 4b-5 and 4b-6 in the text, respectively.

canopy gaps within the smoothed DSM. The best threshold value was determied by trial and error, and 10 m was selected as the threshold value in this study. A similar algorithm of segmenting tree crowns was presented by Hyyppä *et al.* (2001) and Maltamo *et al.* (2003). After generating the individual tree crown outlines, they were laid over both the unsmoothed (i.e., original) DSM and CHM. Subsequently, the predictor variables pertaining to the individual tree crown properties and the tree height used to predict individual stem volumes were calculated from the unsmoothed DSM and CHM, respectively, as mentioned below.

Calculating predictor variables for individual stem volume

Multiple regression was used for predicting the individual stem volumes. Multiplicative models were predicted as linear regressions in the logarithmic variables, because previously, researchers found such models to be suitable for the prediction of volume (Holmgren *et al.* 2003a; Means *et al.* 2000; Næsset 1997). The multiplicative model was formulated as

$$V = \beta_0 H^{\beta 1} CP^{\beta 2} \quad (4b\text{-}1)$$

whereas the linear form used in the equation was

$$\ln V = \ln\beta_0 + \beta_1 \ln H + \beta_2 \ln CP \quad (4b\text{-}2)$$

where V is the field-measured individual stem volume (m^3), H is the LiDAR-derived tree height (m), and CP is the LiDAR-derived crown property. A simple model of single tree and LiDAR-derived crown properties as mentioned below is shown in Fig 4b-1. Moreover, to examine whether the crown properties can essentially improve the accuracy of the predicted individual stem volume together with the LiDAR-derived tree height, two regression models that excluded *CP* from Eqs. 4b-1 and 4b-2 were also used for the prediction of stem volume as follows:

$$V = \beta_0 H^{\beta 1} \quad (4b\text{-}3)$$

$$\ln V = \ln\beta_0 + \beta_1 \ln H \quad (4b\text{-}4)$$

The LiDAR-derived tree height (H : m) was computed as the maximum value of the unsmoothed CHM within the segmented crown (Maltamo *et al.* 2004). Subsequently, we introduced six predictor variables with respect to the individual crown properties in order to predict the individual tree stem volumes in this study. First, the LiDAR-measured crown area (i.e., crown projection area) (*CA*: m^2) was introduced because previously, some researchers found this variable to be a good predictor variable of individual tree stem volumes or stand volume (Holmgren *et al.* 2003a; Hyyppä *et al.* 2001; Means *et al.* 2000; Persson *et al.* 2002). Second, since in Chapter 3 we found that there was a close linear relationship between the stand volume and the LiDAR-estimated sum of sunny crown mantle volume within a stand in hinoki cypress plantations, the LiDAR-estimated sunny crown mantle volume (*SCV*: m^3) for individual trees was also introduced as a predictor variable. *SCV* was calculated as

$$SCV = \sum_{k=1}^{n} a^2 \cdot l_{sck} \quad (4b\text{-}5)$$

where a (m) is the resolution or pixel size of DSM, n is the number of pixels within the segmented individual tree crowns of DSM, and l_{sc} is the estimated vertical depth of the sunny crown mantle. The value of l_{sc} was calculated by subtracting a raster layer, which was derived by applying 3 × 3 minimum filtering to the original DSM, from the original DSM (see Fig 3-1 in Chapter 3). N × N minimum filtering is a type of filtration in which the minimum pixel value within a window of N × N pixels is assigned to the central pixel (Jensen 1996). Since the segmented crown of the original DSM might include pixels associated with canopy gaps, the pixels with l_{sc} values greater than 10 m, as mentioned above, were excluded.

Finally, the other four LiDAR-derived crown properties were the variables with respect to the tree crown form, as mentioned below. Let $P_{i,j}$ denote a pixel (i,j) value within a segmented individual tree crown of the original DSM and P_{max} denote the maximum value of the $P_{i,j}$. Then, crown form (*CF*: m) is denoted as

$$CF = P_{max} - P_{i,j} \quad (4b\text{-}6)$$

Subsequently, statistics of *CF* were calculated for each segmented crown. However, since the segmented crown of the original DSM might include pixels associated with canopy gaps, the pixels with *CF* greater than 10 m were excluded. The value of 10 m was determined by making a decision based on the difference between the threshold value of l_{sc} (10 m) and the field-measured mean tree height (approximately 19-22 m) in this study (Table 4a-2). Subsequently, we introduced four predictor variables named CF_{sum}, CF_{ave}, CF_{sd}, and CF_{cv}, which represent the sum, average, standard

deviation, and coefficient of variation of *CF* within a segmented individual tree crown, respectively.

Regression analysis and validation of the regression model

Prior to regression analysis, each segmented crown (LiDAR-detected crown) had to be identified as the corresponding field stem. If there was only one field stem within a segment, the stem was identified as the segmented crown. If several field stems existed within a crown segment, the stem with the highest tree height value was identified as the segmented crown. Further, the remaining unidentified field stems were considered to be undetected trees using LiDAR data because such trees were relatively smaller than the identified trees.

In the regression analysis, *F*-to-enter, the minimum significance level of a variable to be added, was set at 2.0 and *F*-to-exit was also set at 2.0 (Weisberg 1980). In order to avoid multicollinearity amongst the predictor variables (i.e., between *H* and *CP*), a tolerance limit of the variance inflation factor [VIF = $1/(1 - R_i^2)$] of 10 (Wetherill 1986) was used, where R_i^2 is the multiple correlation of the variable with all other predictor variables in the regression model.

The standard errors of the estimate with original scale ($RMSE_c$: m^3) obtained from Eqs. 4b-2 and 4b-4 were computed as follows:

$$RMSE_c = \sqrt{\frac{\sum_{i=1}^{n}\left(V_i - \hat{V}_i\right)^2}{n - K - 1}} \qquad (4b\text{-}7)$$

where V_i and $\hat{V}_i$ are the field-measured and predicted individual stem volumes (m^3), respectively, and n and K are the number of observations and predictor variables, respectively. In order to ensure that the regression models were not overfitted, a ratio (Q-value) used by Holmgren *et al.* (2003a) was calculated as follows: the standard deviation of the error with logarithmic scale obtained from cross-validation was divided by the standard deviation of the error with logarithmic scale obtained from regression for each model. For cross-validation, we applied the leave-one-out method (Racine 2000). In this study, we performed a regression analysis for each stand and also for the entire site (i.e., three stands were regarded as one stand). This was done in order to investigate which LiDAR-derived crown properties together with the LiDAR-derived tree height estimates can be useful in the regression models to predict individual stem volumes when the difference in stand characteristics and topographical features between the three stands is disregarded.

Results

The number of LiDAR-detected tree crowns that were correctly identified as the corresponding field stem were 126 (69%) in steep slope, 43 (86%) in gentle slope, and 43 (86%) in gentle yet rough terrain (Table 4b-1). Although these percentages of number of detected trees are slightly different from of the Table 4a-4, this difference attributed to which raster data, i.e., CHM (Chapter 4a) and DSM (Chapter 4b), were used for searching local maxima (i.e., tree tops). Moreover, since the minimum number of pixels within crown segments had to be set in LiDAS, this is considered to be one of that reasons. The regression results for the LiDAR-detected trees are shown in Table 4b-2. In this table, the significant level of all regression coefficients except NS (not significant > 0.05) was <0.001. Significantly, all final regression models for the individual stem volume comprised *H* in each stand and the entire site. All crown properties, except CF_{cv} in each stand and the entire site, significantly improved the accuracy of the predicted individual stem volume together with *H*.

The crown properties of the regression models with the highest adjusted coefficient of determination (adjusted R^2) were *SCV* in steep slope, gentle slope, and entire site, and CF_{sum} in gentle yet rough terrain. However, the model with *SCV* had the smallest standard error of the estimate with the original scale (m^3) in each stand and the entire site. The standard errors of the estimate were 0.144 in steep slope, 0.171 in gentle slope, 0.181 in gentle yet rough terrain, and 0.165 in the entire site. These correspond to 23.9%, 21.0%, 20.6%, and 23.6%, respectively, of

Table 4b-1. Number of LiDAR-detected trees, sum of observed volumes for detected trees, and sum of predicted volume for detected trees using regression models with *SCV*[a] in each stand

Stand name	Detected trees[b]	Sum of observed volumes (m^3)[c]	Sum of predicted volumes (m^3)[d]
Steep slope	126 (69%)[f]	75.72 (86%)[f]	74.15 (83%)[f]
Gentle slope	43 (84%)[f]	34.97 (92%)[f]	34.31 (90%)[f]
Gentle yet rough terrain	43 (86%)[f]	37.68 (93%)[f]	36.95 (91%)[f]
Entire site[e]	212 (74%)[f]	148.37 (88%)[f]	144.94 (86%)[f]

[a]*SCV* denotes LiDAR-estimated sunny crown mantle volume calculated using 3×3 minimum filter.

[b]Number of LiDAR-detected trees within each stand.

[c]Sum of observed stem volumes for LiDAR-detected trees within each stand.

[d]Sum of predicted stem volumes for LiDAR-detected trees within each stand.

[e]Entire site denotes all stands.

[f]% denotes the percentage of measures derived from LiDAR against total observed values for all trees within each stand.

Table 4b-2. Regression results where the dependent variable is the individual stem volume with logarithmic scale calculated by using a standard two-way (tree height and diameter at breast height) volume equation

Stand name	Regression model[a]	Regression coefficients[b] $\ln \beta_0$	β_1	β_2	Adjusted R^2	Standard error of the estimate with original scale (m^3)	Q[d]
Steep slope	$\ln \beta_0 + \beta_1 \ln H$	−10.517	3.304		0.689	0.152 (25.4%)[c]	1.01
	$\ln \beta_0 + \beta_1 \ln H + \beta_2 \ln CA$	−9.516	2.768	0.261	0.752	0.145 (24.1%)[c]	1.03
	$\ln \beta_0 + \beta_1 \ln H + \beta_2 \ln SCV$	−9.382	2.738	0.206	0.754	0.144 (23.9%)[c]	1.03
	$\ln \beta_0 + \beta_1 \ln H + \beta_2 \ln CF_{sun}$	−9.919	2.843	0.138	0.736	0.149 (24.8%)[c]	1.02
	$\ln \beta_0 + \beta_1 \ln H + \beta_2 \ln CF_{ave}$	−9.655	2.919	0.246	0.722	0.151 (25.1%)[c]	1.02
	$\ln \beta_0 + \beta_1 \ln H + \beta_2 \ln CF_{sd}$	−9.998	3.078	0.245	0.714	0.151 (25.1%)[c]	1.01
	$\ln \beta_0 + \beta_1 \ln H + \beta_2 \ln CF_{cv}$	−10.517	3.304	NS	0.689	0.152 (25.4%)[c]	1.01
Gentle slope	$\ln \beta_0 + \beta_1 \ln H$	−6.622	2.101		0.387	0.272 (33.4%)[c]	1.03
	$\ln \beta_0 + \beta_1 \ln H + \beta_2 \ln CA$	−5.793	1.310	0.606	0.686	0.196 (24.1%)[c]	1.05
	$\ln \beta_0 + \beta_1 \ln H + \beta_2 \ln SCV$	−7.616	1.965	0.431	0.753	0.171 (21.0%)[c]	1.04
	$\ln \beta_0 + \beta_1 \ln H + \beta_2 \ln CF_{sun}$	−6.809	1.323	0.423	0.674	0.207 (25.5%)[c]	1.04
	$\ln \beta_0 + \beta_1 \ln H + \beta_2 \ln CF_{ave}$	−6.621	1.710	0.871	0.718	0.194 (23.9%)[c]	1.04
	$\ln \beta_0 + \beta_1 \ln H + \beta_2 \ln CF_{sd}$	−7.520	2.160	0.910	0.580	0.224 (27.5%)[c]	1.04
	$\ln \beta_0 + \beta_1 \ln H + \beta_2 \ln CF_{cv}$	−5.616	1.578	−1.017	0.543	0.247 (30.3%)[c]	1.03
Gentle yet rough terrain	$\ln \beta_0 + \beta_1 \ln H$	−9.573	3.009		0.681	0.225 (25.7%)[c]	1.01
	$\ln \beta_0 + \beta_1 \ln H + \beta_2 \ln CA$	−9.124	2.547	0.376	0.781	0.191 (21.8%)[c]	1.03
	$\ln \beta_0 + \beta_1 \ln H + \beta_2 \ln SCV$	−9.616	2.770	0.252	0.777	0.181 (20.6%)[c]	1.04
	$\ln \beta_0 + \beta_1 \ln H + \beta_2 \ln CF_{sun}$	−9.539	2.475	0.271	0.786	0.187 (21.3%)[c]	1.04
	$\ln \beta_0 + \beta_1 \ln H + \beta_2 \ln CF_{ave}$	−9.348	2.746	0.459	0.774	0.185 (21.1%)[c]	1.04
	$\ln \beta_0 + \beta_1 \ln H + \beta_2 \ln CF_{sd}$	−10.049	3.033	0.537	0.776	0.185 (21.1%)[c]	1.04
	$\ln \beta_0 + \beta_1 \ln H + \beta_2 \ln CF_{cv}$	−9.573	3.009	NS	0.681	0.225 (25.7%)[c]	1.01
Entire site	$\ln \beta_0 + \beta_1 \ln H$	−9.427	2.964		0.614	0.207 (29.6%)[c]	1.01
	$\ln \beta_0 + \beta_1 \ln H + \beta_2 \ln CA$	−8.312	2.282	0.389	0.734	0.178 (25.5%)[c]	1.02
	$\ln \beta_0 + \beta_1 \ln H + \beta_2 \ln SCV$	−8.634	2.411	0.301	0.765	0.165 (23.6%)[c]	1.02
	$\ln \beta_0 + \beta_1 \ln H + \beta_2 \ln CF_{sun}$	−8.936	2.361	0.230	0.713	0.186 (26.6%)[c]	1.01
	$\ln \beta_0 + \beta_1 \ln H + \beta_2 \ln CF_{ave}$	−8.613	2.511	0.448	0.711	0.184 (26.4%)[c]	1.01
	$\ln \beta_0 + \beta_1 \ln H + \beta_2 \ln CF_{sd}$	−9.107	2.752	0.458	0.688	0.189 (27.0%)[c]	1.01
	$\ln \beta_0 + \beta_1 \ln H + \beta_2 \ln CF_{cv}$	−8.948	2.729	−0.429	0.635	0.205 (29.3%)[c]	1.01

[a] H, CA and SCV denote LiDAR-derived tree height, crown area and estimated sunny crown mantle volume caluculated using 3×3 mimimum filter. CF denotes crown form expressed by the LiDAR-derived height value and four subscripts refer to the sum, average, standard deviation, and coefficient of variation, respectively which are calculated with the LiDAR-derived height value.

[b] Significant level of all regression coefficients was < 0.001 except NS. NS = not significant (> 0.05)

[c] The percentage corresponds to the error percentage of average individual stem volume.

[d] Q-value is calculated as the standard deviation of the error for cross-validation divided by the standard deviation of the error obtained from regression.

the average field-measured stem volume for LiDAR-detected trees. The Q-values of all regression models were nearly equal to one, and this indicates that all the models were not overfitted. The relationship between the field-measured and predicted individual stem volumes with the smallest standard error of the estimate for each stand is shown in Fig 4b-2.

Sums of the individual stem volume for detected trees that were predicted by the regression model with *SCV* in each stand and the entire site are shown in Table 4b-2. The sum of the predicted volumes was slightly underestimated in each stand and the entire site; however, the differences between the field-measured volumes and predicted volumes were only 1-3% for the detected trees. The percentages of the sum of predicted volumes in each stand and the entire site were greater than the percentages of the number of detected trees.

Discussion

One of the main objectives of this study was to investigate which predictor variables with respect to crown properties, derived from the LiDAR data together with the LiDAR-derived individual tree height (*H*) could be useful in regression models to predict the individual stem volumes of sugi for each stand that has different stand characteristics with different topographical features in mountainous forests. Essentially, most crown properties could

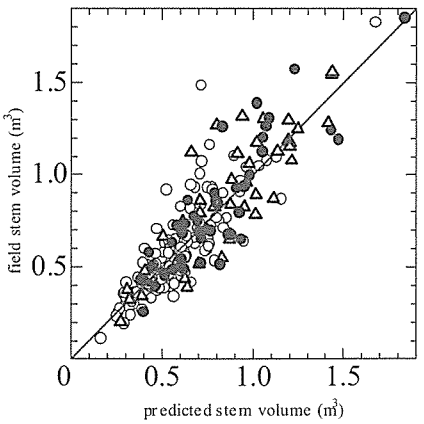

Fig 4b-2. The relationship between field-measured and predicted individual stem volumes. Black and white circles and triangles denote the LiDAR-detected trees in steep and gentle slope, and gentle yet rough terrain, respectively.

improve the accuracy of the predicted individual stem volume together with *H* in each stand and the entire site (Table 4b-2). Particularly in gentle slope, the adjusted R^2 value of Eq. 4b-2 was greatly improved from 0.378 to 0.753, with the highest value obtained in Eq. 4b-4. The field-measured individual stem volumes were calculated from a standard two-way volume equation using the tree height and the DBH. Therefore, the LiDAR-derived crown properties might significantly explain the stem volumes instead of the DBH in this study because *H* used in Eqs. 4b-2 and 4b-4 were found to be accurate in each stand in Chapter 4a.

Holmgren *et al.* (2003a) have shown that tree height and crown area were the LiDAR-derived predictor variables that proved significant for predicting the plot level stem volume for coniferous forests. In this study, *H* and *CA* were also significant variables for predicting the individual stem volume. Moreover, both *CA* and *SCV* and the other three crown properties with respect to the crown form (CF_{sum}, CF_{ave}, and CF_{sd}) were revealed as significant predictor variables for predicting the individual stem volume in each stand and the entire site by regression analysis. In addition, it was ensured that each model was not overfitted and was considered to be a stable model because the Q-value of all models was nearly one. The regression model with the smallest standard error of the estimate with the original scale was the model with *SCV* in each stand and the entire site. Thus, considering all factors, the model with *SCV* would be the best of the six models of each stand and the entire site in this study. This indicates that the *SCV* together with *H* would be able to greatly explain the individual stem volumes regardless of the different topographical features and stand characteristics such as stand density, the mean tree height and crown radius, etc., at least in even-aged sugi plantations in mountainous areas.

The sums of the individual stem volume for detected trees, predicted by the regression model with *SCV*, were slightly underestimated (1-3%) in each stand and the entire site (Table 4b-1). Approximately 70-85% of the total number of trees was correctly detected using the LiDAR data. However, the sum of stem volumes predicted by the regression model with *SCV* for the detected trees in this study occupied over 80-90% of the total field-measured stem volumes for all trees within each stand. The results in this study indicated that a large portion of the LiDAR-detected trees had larger individual stem volume than the undetected trees in each stand and the entire site. The approach of only summing the predicted individual stem volumes for LiDAR-detected trees in this study led to underestimation of the stand volume, similar to that shown by Persson *et al.* (2002) and Yone *et al.* (2002). This is because small-footprint airborne LiDAR data offered the possibility to detect most canopy trees and hardly any sub-canopy trees of smaller height, such as suppressed or intermediate trees (Holmgren *et al.* 2003a; Maltamo *et al.* 2004; McCombs *et al.* 2003; Persson *et al.* 2002; Yone *et al.* 2002). Unlike the approach to predict stand volume by summing the predicted individual stem volumes of LiDAR-detected trees, other researchers previously used height distribution of laser height measurements in combination with density-related variables, such as the proportion of laser returns from the canopy, to predict stand volume (e.g., Means *et al.* 2000; Næsset 2002). Since the sum of all tree stem volumes within a stand is regressed against the measures of the laser canopy height distributions and the density-related variables, such a method would produce fewer underestimates than the approach used in this study. However, according to Holmgren *et al.* (2003b), simulations showed that laser height percentiles and the proportion of canopy returns changed more with an increased scanning angle for long crown species, such as spruce, in comparison with short crown species such as pine. This indicates that each regression model for predicting each forest parameter such as mean tree height, basal area, and stand volume might have different predictor variables in the different settings of LiDAR systems or forest types. Therefore, collecting information regarding individual tree parameters to predict forest parameters might be more useful for detailed forestry monitoring and forest management. Methods that use the information of individual tree parameters for LiDAR-detected canopy trees should be developed if we want to predict the stand volume more accurately. For example, Yone *et al.* (2002) indicated that a method using aerial stand volume tables for LiDAR data would provide the best results for estimating stand volume since such tables had been prepared to estimate volume including both visible and invisible trees. Maltamo *et al.* (2004) used theoretical distribution functions to predict the number of stems and stem volume for suppressed trees accurately, and they showed that their approaches improved the underestimation of stem density and stand volume. However, both methods were insufficient for predicting actual stand volume; therefore, we need

to develop these methods or investigate better procedures for predicting accurate stand volumes in the future.

The results of this study indicated that small-footprint airborne LiDAR will be a useful tool for predicting the individual stem volume for LiDAR-detected trees and the stand volume of sugi plantations in mountainous areas. LiDAR-estimated sunny crown mantle volume would be as good as or a better predictor variable than the LiDAR-derived crown area in case of regression, together with the LiDAR-derived tree height, for predicting the individual stem volumes of sugi plantations for LiDAR-detected trees regardless of the different topographical features and stand characteristics in mountainous forests.

Chapter 5. General Discussion

The development of a system for the measurement of forest attributes in coniferous mountainous forests consisting mainly of middle-aged sugi and hinoki cypress plantations in Japan using small-footprint airborne LiDAR required considerable research. As mentioned previously, one of the objectives of this study was to focus on accurate assessments of tree height because tree height is one of the most significant parameters in forest measurement. Since accurate DTMs usually facilitate equally accurate estimations of tree height in LiDAR remote sensing, first the possibility to create accurate DTM was examined for sugi and hinoki cypress stands in Chapter 2. As expected, the low penetration rate of LiDAR pulses (1.1%) in hinoki cypress stands, which was approximately one eighth of that of the sugi stand, meant that creation of an accurate DTM was not possible and neither were examined in the hinoki cypress stand. However, the generation of a DTM and estimation of tree height were examined in the sugi stand and these are covered in Chapters 3 and 4, respectively. The differences in penetration rate of the LiDAR pulses in each stand is a general attribute of each stand and confers the ability to discriminate between sugi and hinoki cypress stand efficiently using penetration rate as an indicator. This information can then subsequently be used to select the appropriate procedure for estimating forest parameters as described in Chapter 3 and 4, respectively.

For DTM creation, some researchers have suggested that, although filters have not used the recorded pulse reflectance strengths, neither have they used aerial photographs or maps to support the separation of LiDAR data into vegetation data and ground data, such additional information on a scene (fusion of data) could potentially provide a much better understanding of a scene and thereby improve filter performance (Ackermann 1999; Axelsson 1999; Sithole and Vosselman 2004). Although fusion of several kinds of data should be attempted when creating a DTM in areas with low LiDAR pulse-penetration rates, we propose the development of a new method based on the idea of the *top surface model* proposed in Chapter 2. Since the *top surface model* can reflect the ground surface, at least in a small area, we might be able to create accurate DTM combining the LiDAR pulse data that hit the ground with the *top surface model* and this will serve as the basis for future work. As reported by Sithole and Vosselman (2004) in their assessment of the performance of several filters (i.e., methodologies and algorithms for creating DTMs), all filters performed well in smooth rural landscapes, but all filters produced errors in structurally complex urban areas and over rough terrain with vegetation despite. However, good estimates of DTM data were acquired for the sugi stand in the mountainous areas examined in this study by applying a filter developed by Holmgren *et al.* (2003a) with spline interpolation (Magnussen and Boudewyn 1998; Magnussen *et al.* 1999; Riaño *et al.* 2003; Brovelli *et al.* 2004) (Chapter 4a), although another methods should also be tested in order to determine the best method for creating DTMs in those areas.

The procedures for estimating forest parameters presented in Chapter 3 and 4 are based on mainly raster-based analysis. Since the volumes of raw LiDAR point data are considerable, and relatively modest datasets are composed of millions or tens of millions of returning pulses (St-Onge *et al.* 2003), the conversion of 3-D point clouds into 2-D raster data can reduce the volumes significantly and facilitate data processing. Moreover, we can apply image processing techniques that are capable of using the neighborhood information of points, clouds and pixels characteristic of DSM and CHM data, more efficiently. Physical features, such as tree crowns, individual trees, groups of trees, or whole forest stands, can be delineated using image processing techniques before being analyzed using existing models to estimate forest and stand parameters (Hyyppä *et al.* 2004). For example, the local maximum filtering for detecting individual tree tops, minimum filtering for calculating vertical crown depth, and segmentation of individual tree crowns presented in this study do not require 3-D point data, only 2-D raster data. Therefore, a raster-based system for forest measurement using small-footprint airborne LiDAR would be useful since we can extract the tree information on both the individual and stand level, although sub-canopy tree information cannot be acquired.

Some researchers have used laser height percentiles of the distribution of canopy heights as predictor variables and density-related variables, such as the proportion of laser returns from the canopy, in regression models for estimation of mean tree height, basal area and stand volume (Magnussen *et al.* 1999; Means *et al.* 2000; Næsset and Bjerknes 2001; Næsset and Økland 2002; Næsset 2002; Popescu *et al.* 2002, 2003). Such statistical methods, mainly based on stepwise regression analysis have the advantage of being applied directly to forest parameters at stand or plot level, and are highly likely to produce the regression models with high coefficients of determination (R^2) since stepwise regression often

selects many predictor variables within each model. Moreover, since this approach is mainly applied to 3-D point data, sub-canopy tree information may be included in the statistic and good estimates of stand volume (R^2 = 0.95-0.97) derived using this method have been reported (Means *et al.* 2000). However, the resultant models cannot be widely applied because, as shown in the simulations of Holmgren *et al.* (2003b) discussed in Chapter 4b, each regression model for predicting each forest parameter might have predictor variables that might vary between different of LiDAR system settings or forest types. This is particularly important given that the evolution of LiDAR technology will continue to enhance data quality and richness (Lim *et al.* 2003) and this may greatly affect the resultant LiDAR-derived predictor variables in each regression model of forest parameters (e.g., the variety of the laser height percentiles of the distribution of canopy heights and the proportion of laser returns from the canopy). Conversely, a raster-based approach can usually produce direct measurements (estimates) of physical features corresponding to dependent variables regardless of the differences in LiDAR measurement settings.

Since small-footprint airborne LiDAR can only characterize objects based on their 3-D coordinates (*X*, *Y*, *Z*) and does not produce colorful images that contain spectral information of the objects they describe, it is difficult to classify tree species using LiDAR data alone. However, Holmgren and Persson (2004) demonstrated how airborne laser scanning of the structure and shape of tree crowns could be used discriminate between Norway spruce (*Picea abies* L. Karst) and Scots pine (*Pinus sylvestris* L.) on an individual tree level and with high accuracy. In their report, only two species could not be discriminated between, but this is a limitation common to all species surveys (i.e., accurate identification to species-level and species number itself are inversely proportional). Persson *et al.* (2004) subsequently attempted species identification (also in Norway spruce and Scots pine, as above, and in deciduous trees) and found that the combination of high resolution laser data with high resolution near-infrared images increased the accuracy species identification and that near-infrared images add useful information for tree species classification. These studies demonstrated that, although it is difficult to classify tree species using only LiDAR data, fusion and combining passive optical remotely sensed data with LiDAR data have considerable potential in accurately measuring and monitoring forests. Since the combination of small-footprint airborne LiDAR with passive optical remote sensing techniques for forest measurements is a relatively new technique, particularly in Japan, this should be explored further to improve our forest measurement capabilities presented in this study and beyond. For example, we must be able to discriminate sugi and hinoki cypress on the stand-level or individual tree-level efficiently and automatically.

The procedures for measuring individual canopy (predominant) tree heights adopted by three studies in Japan (Yone *et al.* (2002), Omasa *et al.* (2003) and this study), were all based on raster-based analysis, and the accuracy of the LiDAR-derived tree height estimates (RMSE) was less than 1 m in all three studies. The results of these studies indicate that small-footprint airborne LiDAR is a useful tool in the measurement of tree height, at least in middle-aged sugi and Japanese larch plantations in Japan. Although these studies also estimate individual stem volumes or carbon stocks for LiDAR-detected trees, this was done using procedures that varied between the respective studies. For example, field-measured stem volumes were regressed against LiDAR-derived tree heights and sunny crown mantle volume (this study), stem volumes were estimated by empirical height-volume equation (Yone *et al.* 2002), and carbon stocks of trees were estimated by empirical height-carbon stocks equation (Omasa *et al.* 2003). Since a comparative study of these methods has not been yet been undertaken, it is not possible to suggest at present which method is best suited to estimating stem volumes and carbon stocks. However, at least it has been conclusively demonstrated that tree height can be measured directly using small-footprint airborne LiDAR. It therefore seems likely that we will be able to apply the technique to estimate tree height accurately in middle-aged sugi and Japanese larch plantations on the regional scale needed for cross-checking carbon stocks and for sink accounting in a transparent and verifiable manner in accordance with the QA/QC guidelines of the Kyoto Protocol. We will also have the ability to measure canopy tree heights using airborne remote sensing techniques objectively and efficiently on a regional scale compared that currently possible by crews on the ground.

In Japan, the application of small-footprint airborne LiDAR remote sensing for forest measurement has just begun and the studies into the potential for the technology and methods is currently insufficient. The potential of this powerful technique should be investigated and evaluated further through research conducted in other forest areas. Moreover, we particularly need to develop procedures for creating DTMs accurately in hinoki cypress stands in order to measure and estimate tree heights accurately using mainly small-footprint airborne LiDAR. Although there is still much to be done regarding the application of small-footprint airborne LiDAR given its high potential for forest measurement, I hereby propose that a system for forest measurement, especially one directed at the estimation of tree height and stand volume in mountainous coniferous forests consisting mainly of sugi (*Cryptomeria japonica* D. Don) and hinoki cypress (*Chamaecyparis obtusa* Sieb. et Zucc.) be undertaken using small-footprint airborne LiDAR based on the results obtained in this study in the following way. First, we need to acquire accurate distribution data for sugi and hinoki cypress

stands using passive optical remote sensing data, such as geometrically corrected digital aerial photographs, or manually or semi-automatically classified multi-spectral images before we analyze LiDAR data. If we want to obtain individual tree information, LiDAR data acquisition should be performed using settings with similar footprint diameter and high sampling density so as to be at least greater than or equal to 4 to 5 points/m2. This can then be used to produce a DSM with a resolution of 0.3 m to 0.5 m as recommended in this study. After selecting the appropriate LiDAR data for each stand and combining it with the digital spectral images on a computer using GIS, we should estimate stand volume in hinoki cypress stands, individual tree height, stem volume and stand volume can then be calculated in the sugi stands using the methods presented in Chapter 3 and 4, respectively.

Acknowledgments

I would like to express my sincere gratitude to Associate professor Kazukiyo Yamamoto and Professor Chisato Takenaka for their devoted guidance, pertinent advice throughout this Ph. D study. Furthermore I wish to thank the teaching staff at the Nagoya University experimental forest and Yosuke Miyachi, Mie Miyahara and Shoko Ogawa who conducted some of the fieldwork and all members of the author's laboratory for help and many valuable suggestions during this study.

In conclusion, I especially appreciate Emeritus professor of Nagoya University; Takeo Umemura, Dr. Rie Tomioka, Emeritus professor of Nagoya University; Osafumi Tezuka, and thank to my family and many good friends for support and encouragement that allowed me to accomplish this study.

References

Ackermann F (1999) Airborne laser scanning: present status and future expectations. *ISPRS J Photogramm Rem Sens* 54: 64-67

Axelsson P (1999) Processing of laser scanner data-algorisms and applications. *ISPRS J Photogramm Rem Sens* 54: 138-147

Baltsavias EP (1999a) A comparison of between photogrammetry and laser scanning. *ISPRS J Photogramm Rem Sens* 54: 83-94

Baltsavias EP (1999b) Airborne laser scanning: existing systems and firms and other resources. *ISPRS J Photogramm Rem Sens* 54: 164-198

Brandtberg T, Warner TA, Landenberger RE, McGraw JB (2003) Detection and analysis of leaf-off tree crowns in small footprint, high sampling density lidar data from the eastern deciduous forest in North America. *Rem Sens Environ* 85: 290-303

Brovelli MA, Cannata M, Longoni UM (2004) LIDAR data filtering and DTM interpolation within GRASS. *Trans GIS* 8: 155-174

Cowen DJ, Jensen JR, Hendrix C, Hodgson ME, Schill SR (2000) A GIS assisted rail construction econometric model that incorporates LIDAR data. *Photogramm Eng Rem Sens* 66: 1323-1328

Gundimeda H (2004) How 'sustainable' is the 'sustainable development objective' of CDM in developing countries. *For Poli Econ* 6: 329-343

Elmqvist M (2000) Automatic ground modeling using laser radar data. Masters thesis LiTH-ISY-EX-3061, Dep Elect Eng, Linköping Univ, Linköping, Sweden, 3-30 pp

Evans DL, Roberts SD, McCombs JW, Harrington RL (2001) Detection of regularly spaced targets in small-footprint LIDAR data: Research issues for consideration. *Photogramm Eng Rem Sens* 67: 1133-1136

Forestry Agency (1970) Timber volume table (Western Japan) (in Japanese). Nihon Ringyo Chosakai, Tokyo, Japan, pp 13

Fujisawa H (2004) The forest planning system in relation to the forest resource and forestry policies. *J For Res* 9: 1-5

Gaveau DLA, Hill RA (2003) Quantifying canopy height underestimation by laser pulse penetration in small-footprint airborne laser scanning data. *Can J Rem Sens* 29: 650-657

Hattori S, Abe T, Kobayashi C, Tamai K, (1992) Effect of forest floor coverage on reduction of soil erosion in hinoki cypress plantations (in Japanese with English summary). *Bull Forestry and Forest Products Research Institute* 362: 1-34

Heurich M, Schneider T, Kennel E (2003) Laser scanning for identification of forest structures in the Bavarian Forest National Park. Proceedings of ScandLaser, 2-4 September, Umeå, Sweden 97-106

Hirata Y, Sato K, Shibata M, Nishizono T (2003) The capability of helicopter-borne laser scanner data in a temperate deciduous forest. Proceedings of ScandLaser, 2-4 September, Umeå, Sweden 174-179

Hirata Y (2004) Three-dimensional forest measurement with airborne laser scanner (in Japanese). *J Jpn Soc Civ Eng* 89: 28-30

Hodgson ME, Jensen JR, Schmidt L, Schill S, Davis B (2003) An evaluation of LIDAR- and IFSAR-derived digital elevation models in leaf-on conditions with USGS Level 1 and Level 2 DEMs. *Rem Sens Environ* 84: 295-308

Holmgren J, Nilssson M, Olsson H (2003a) Estimation of tree height and stem volume on plots using airborne laser scanning. *For Sci* 49: 419-428

Holmgren J, Nilssson M, Olsson H (2003b) Simulating the effects of lidar scanning angle for estimation of mean tree height and canopy closure. *Can J Rem Sens* 29: 623-632

Holmgren J, Persson Å (2004) Identifying species of individual trees using airborne laser scanner. *Rem Sens Environ* 90: 415-423

Hyyppä J, Inkinen M (1999) Detecting and estimating attributes for single trees using laser scanner. *Photogramm J Finland* 16: 27-42

Hyyppä J, Hyyppä H, Inkinen M, Engdahl M, Linko S, Yi-Hong, Z (2000) Accuracy comparison of various remote sensing data sources in the retrieval of forest stand attributes. *For Ecol Man* 128: 109-120

Hyyppä J, Kelle Olavi, Lehikoinen M, Inkinen M (2001) A segmentation-based method to retrieve stem volume estimates from 3-D tree height models produced by laser scanners. *IEEE Trans Geosci Rem Sens* 39: 969-975

Hyyppä J, Hyyppä H, Litkey P, Yu X, Haggrén H, Rönnholm P, Pyysalo U, Pitkänen J, Maltamo M (2004) Algorithms and methods of airborne laser scanning for forest measurements. *Int Arc Photogramm, Rem Sens and Spatial Info Sci* 36: part8/w2

IPCC (Intergovernmental Panel on Climate Change) (2004) Good Practice Guidance for Land Use and Land-Use Change and Forestry. IGES

Japan Forestry Association (2003) Annual report on trends of forest and forestry (in Japanese). Nihon Ringyo Kyokai, Tokyo, Japan

Jensen JR, Hodgson ME, Mackey JrHE, Krabill W (1987) Correlation between aircraft MSS and LiDAR remotely sensed data on a forested wetland. *Geocarto International* 4: 39-54

Jensen JR (1996) Introductory digital image processing, 2nd ed. Prentice-Hall, NJ, pp 154-158

Kajihara M (1981a) Crown form, crown structure and the relationship between crown dimensions and leaf fresh weight of Hinoki cypress (*Chamaecyparis obtusa*). *Bull Kyoto Pref Univ For* 25: 11-28

Kajihara M (1981b) Vertical distibution of stem volume increment and its model relating to crown position in Sugi (*Cryptomeria japonica*) and Hinoki cypress (*Chamaecyparis obtusa*). *The Scientific Reports of Kyoto Pref Univ Agri* 33: 63-72

Kajihara M (1982) Relationship between Crown Dimensions and Stem Volume Increment in Sugi (*Cryptomeria japonica*) and Hinoki cypress (*Chamaecyparis obtusa*). *Bull Kyoto Pref Univ For* 26: 16-23

Kraus K, Pfeifer N (1998) Determination of terrain models in wooded areas with airborne laser scanning data. *ISPRS J Photogramm Rem Sens* 53: 193-203

Leckie D (1990) Advances in remote sensing technologies for forest survey and management. *Can J For Res* 20: 464-483

Leckie D, Beaubien J, Gibson J, O'Niell N, Piekutowski T, Joyce S (1995) Data processing and analysis for MIFUCAM: a trial for MEIS imagery for forest inventory mapping. *Can J Rem Sens* 21: 337-356

Lefsky MA, Cohen WB, Spies TA (2001) An evaluation of alternate remote sensing products for forest inventory, monitoring, and mapping of Douglas-fir forests in western Oregon. *Can J For Res* 31: 78-87

Lim K, Treitz P, Wulder M, St-Onge B, Flood M (2003) LiDAR remote sensing of forest structure. *Prog Pysi Geo* 27: 88-106

Maclean GA, Krabill WB (1986) Gross-merchantable timber volume estimation using an airborne Lidar system. *Can J Rem Sens* 12: 7-18

Magnussen S, Boudewyn P (1998) Derivations of stand heights from airborne laser scanner data with canopy-based quantile estimators. *Can J For Res* 28: 1016-1031

Magnussen S, Eggermont P, LaRiccia VN (1999) Recov-ering tree heights from airborne laser scanner data. *For Sci* 45: 407-422

Maltamo M, Tokola T, Lehikoinen M (2003) Estimating stand characteristics by combining single tree pattern recognition of digital video imagery and a theoretical diameter distribution model. *For Sci* 49: 98-109

Maltamo M, Eerikäinen K, Pitkänen J, Hyyppä J, Vehmas M (2004) Estimation of timber volume and stem density based on scanning laser altimetry and expected tree size distribution functions. *Rem Sens Environ* 90: 319-330

Matsumoto M (2001) Carbon stock and carbon sink in forests in Japan (in Japanese). *SHINRIN KAGAKU* 33: 30-36

Matsumoto M (2005) Grappling with the development of the carbon accounting system under the Kyoto Protocol (in Japanese). *SHINRIN GIJUTSU* 759: 3-9

McCombs JW, Roberts SD, Evans DL (2003) Influence of fusing lidar and multispectral imagery on remotely sensed estimates of stand density and mean tree height in a managed loblolly pine plantation. *For Sci* 49: 457-466

Means JE, Acker SA, Harding DJ, Blair JB, Lefsky MA, Cohen WB, Harmon ME, McKee WA, (1999) Use of large-footprint scanning airborne LiDAR to estimate forest stand characteristics in the western cascades of Oregon. *Rem Sens Environ* 67: 298-308

Means JE, Acker SA, Fitt BJ, Renslow M, Emerson L, Hendrix CJ (2000) Predicting forest stand characteristics with airborne scanning LiDAR. *Photogramm Eng Rem Sens* 66: 1367-1371

Næsset E (1997a) Determination of tree height of forest stands using airborne laser scanner data. *ISPRS J Photogramm Rem Sens* 52: 49-56

Næsset E (1997b) Estimating timber volume of forest stands using airborne laser data. *Rem Sens Environ* 61: 246-253

Næsset E, Bjerknes K O (2001) Estimating tree heights and number of stems in young forest stands using airborne laser scanner data. *Rem Sens Environ* 78: 328-340

Næsset E, Økland T (2002) Estimating tree height and tree crown properties using airborne scanning laser in a boreal nature reserve. *Rem Sens Environ* 79: 105-115

Næsset E (2002) Predicting forest stand characteristics with airborne scanning laser using a practical two-stage procedure and field data. *Rem Sens Environ* 80: 88-99

Nelson R, Krabill W, Tonelli J (1988) Estimating forest biomass and volume using airborne laser data. *Rem Sens Environ* 24: 247-267

Niblack W, (1986) An introduction to digital image processing. Prentice-Hall, Englewood Cliffs, N.J., pp 115-116

Nilsson M (1996) Estimation of tree height and stand volume using an airborne LiDAR system. *Rem Sens Environ* 56: 1-7

Omasa K, Qui GY, Watanuki K, Yoshimi K, Akiyama Y (2003) Accurate estimation of forest carbon stocks by 3-D remote sensing of individual trees. *Environ Sci Technol* 37: 1198-1201

Otsu N, (1979) A threshold selection method from grey-level histograms. *IEEE Trans Systems, Man and Cybernetics* 9: 62-66

Persson Å, Holmgren J, Soderman U (2002) Detecting and measuring individual trees using an airborne laser scanner. *Photogramm Eng Rem Sens* 68: 925-932

Persson Å, Holmgren J, Soderman U, Olsson H (2004) Tree species classification of individual trees in Sweden by combining high resolution laser data with high resolution near-infrared digital images. *Int Arc Photogramm, Rem Sens and Spatial Info Sci* 36: part8/w2

Peter N (2004) The use of remote sensing to support the application of multilateral environmental agreements. *Space poli* 20: 189-195

Pfeifer N, Gorte B, Elberink SO (2004) Influences of vegetation on laser altimetry: analysis and correction approaches. *Int Arc Photogramm, Rem Sens and Spatial Info Sci* 36: part8/w2

Popescu SC, Wynne RH, Nelson RF (2002) Estimating plot-level tree heights with lidar: local filtering with a canopy-height based variable window size. *Com Elect Agr* 37: 71-95

Popescu SC, Wynne RH, Nelson RF (2003) Measuring individual tree crown diameter with lidar and assessing its influence on estimating forest volume and biomass. *Can J Rem Sens* 29: 564-577

Racine J (2000) Consistent cross-validatory model-selection for dependent data: *hv*-block cross-validation. *J Econ* 99: 39-61

Riaño D, Meier E, Allgöwer B, Chuvieco E, Ustin SL (2003) Modeling airborne laser scanning data for the spatial generation of critical forest parameters in fire behavior modeling. *Rem Sens Environ* 86: 177-186

Rignot E, Way J, Williams C, Viereck L (1994) Radar estimates of aboveground biomass in boreal forests of interior Alaska. *IEEE Trans Geosci Rem Sens* 32: 1117-1124

Ritchie JC, Everitt JH, Escobar TJ, Davis MR (1992) Airborne laser measurements of rangeland canopy cover and distribution. *J Range Manage* 45: 189-193

Ritchie JC, Evans DL, Jacobs D, Everitt JH, Weltz MA (1993) Measuring canopy structure with an airborne laser altimeter. *Trans ASAE* 36: 1235-1238

Rosenqvist Å, Milne A, Lucas R, Imhoff M, Dobson C (2003) A review of remote sensing technology in support of the Kyoto Protocol. *Environ Sci Poli* 6: 441-455

Sekine H, Yamagata Y, Oguma H (2002) The monitoring of ARD activities for sink project area using satellite data. *J Rem Sens Soc Jpn* 22: 517-530

Sithole G, Vosselman G (2004) Comparison of filtering algorithms. *Int Arc Photogramm, Rem Sens and Spatial Info Sci* 35: part3/w13

St-Onge B, Treitz P, Wulder MA (2003) Tree and canopy height estimation with scanning lidar. In: *Remote sensing of forest environments: Concepts and case studies* (Wulder MA and Franklin SE eds). pp 489-509. Kluwer Academic Publishers, Boston

Suematsu Y, Yamada H (2000) Image processing engineering (in Japanese). Corona Publishing, Tokyo, Japan, pp 120-121

Takahashi T, Yamamoto K, Takenaka C, Umemura, T (2000) The effect of topographical factors on tree height growth (in Japanese with English summary). *Nagoya Univ For Sci* 19: 49-53

Takeda H (2004) Ground surface estimation in dense forest. *Int Arc Photogramm, Rem Sens and Spatial Info Sci* 35: partB3 1016-1023

Weisberg S (1980) Applied linear regression. John Wiley & Sons, New York, pp 86-243

Wetherill GB (1986) Regression analysis with applications. Chapman and Hall, London, pp 154-158

Wulder M (1998) Optical remote-sensing techniques for the assessment of forest inventory and biophysical parameters. *Prog Pysi Geo* 22: 449-476

Wulder M, Niemann KO, Goodenough DG (2000) Local maximum filtering for the extraction of tree locations and basal area from high spatial resolution imagery. *Rem Sens Environ* 73: 103-114

Yamagata Y, Yamada K (2000) International trends in sink-related projects under the Kyoto Protocol (in Japanese). CGER Report (CGER-D027-2000), Tsukuba, Japan

Yamagata Y, Oguma H, Tsuchida S, Sekine H, Rokugawa S (2001) The role of remote sensing for monitoring and verification of the carbon sinks under the Kyoto Protocol (in Japanese with English summary). *J Rem Sens Soc Jpn* 21: 43-57

Yamagata Y, Ishii A (2001) Sinks under the Kyoto Protocol: Bonn Agreement and its political implicature (in Japanese). CGER Report (CGER-D029-2001), Tsukuba, Japan

Yamagata Y, Oguma H, Sekine H, Tsuchida S (2002) The role of remote sensing for monitoring the carbon sink activities (in Japanese with English summary). *J Rem Sens Soc Jpn* 22: 494-509

Yone Y, Oguma H, Yamagata Y (2002) Development of measurement system for the carbon sinks under the Kyoto protocol (in Japanese with English summary). *J Rem Sens Soc Jpn* 22: 531-543

Zimble DA, Evans DL, Carlson GC, Parker RC, Grado SC, Gerard PD (2003) Characterizing vertical forest structure using small-footprint airborne LiDAR. *Rem Sens Environ* 87:171-182

Summary

Small-footprint LiDAR remote sensing techniques have been anticipated as a useful tool to acquire forest parameters in detail. However, the detail researches for application of small-footprint airborne LiDAR to forest measurements in Japan are only some plantations with flat terrain. Therefore, if we wan to use it practically for cross-checking of the accounted carbon stock and sink in FM activities under the Kyoto Protocol, it must be proved the ability of small-footprint airborne LiDAR to measure and monitor mountainous coniferous forests because in Japan, there exist many dense coniferous forests consisted of sugi (*Cryptomeria japonica* D. Don) and hinoki cypress (*Chamaecyparis obtusa* Sieb. et Zucc.) plantations which have not been adequately thinned and weeded in mountainous areas, the topography of which is likely to be steeper and more complex than that of previously researched sites. Thereby, we investigated the potential of small-footprint airborne LiDAR for forest measurement in such mountainous coniferous forests in detail.

Firstly, in order to know the characteristics of penetration rates of laser pulses transmitted from a small-footprint airborne LiDAR system in both sugi and hinoki cypress stands, we investigated it in a middle-aged (40-50 year old) hinoki cypress and sugi plantation that had similar levels of canopy openness. The number of transmitted pulses was 107,427 points/ha for the hinoki cypress stand and 122,883 points/ha for the sugi stand. The penetration rate of the first pulse (P_f) and second pulse (P_s) that hit the ground was 0.1% and 1.0%, respectively in the hinoki cypress stand and 2.6% and 5.5% in the sugi stand, respectively. That is, the penetration rate of total pulses (P_{f+s}) that hit ground within each stand was 1.1% and 8.1%, respectively. According to a statistical significant test for the difference between the two population proportions, there was a significant difference for each penetration rates (i.e., P_{f+s}, P_f, and P_s) between sugi and hinoki cypress stand ($p < 0.001$). The results indicated that it may be difficult to create an accurate DTM in middle-aged hinoki cypress stands that have been improperly managed, such as this study area, by using only the information on the data of the LiDAR pulses that exhibited poor penetration and hit the ground. Therefore, we found that method of forest measurement using LiDAR for sugi and hinoki cypress stands in mountainous areas should be conducted separately.

According to the results of the investigation of the penetration rates of laser pulses, we found that a DTM cannot always be generated easily and accurately in every forest stand, especially in hinoki cypress stand. Therefore, a procedure for estimating stand volume without generating and using the DTM created by mainly last pulse data, which is equal to second pulse data in this study, should be developed. Such a procedure would free us from the troublesome post processing procedures that use last pulse data to generate an accurate DTM. Therefore in the next study, we proposed a new single predictor variable for directly estimating stand volume in hinoki cypress stands without estimating and using the DTM and the tree height. The variable can easily be extracted using only first pulse data without generating and using a DTM. We also demonstrated the applicability of this variable by use of ground truth data of hinoki cypress plantations. The variable corresponds to sunny crown mantle volume and was calculated using only first pulse data acquired from small-footprint LiDAR. This predictor variable was highly correlated with observed stand volume in 72-year-old and 16-year-old hinoki cypress plantations. Moreover, according to the regression analysis, the simplest relationship between the variable and observed stand volume was expressed as a simple ratio ($p < 0.01$; $R^2=0.922$). The importance of this variable is that unlike LiDAR-derived height-based variables previously presented it does not require the computational procedure of generating an accurate DTM. Thus, this single predictor variable offers a convenient and accurate method of estimating stand volume in hinoki cypress stands.

Next, we investigated the usefulness of LiDAR measurement for sugi stands in detail more than hinoki cypress stands because we have a possibility to be able to create accurate DTM in sugi stands. Since most of the areas studied previously were limited to only flat terrain, we investigated the accuracy of LiDAR-derived individual tree height estimates for different types of topographical features in mountainous forests with a steeper and more complex topography. We chose 48-year-old sugi plantations to investigate the accuracy of these estimates. The surveyed area was divided into three types of topographical features; steep slope (mean slope ± SD; 37.6° ± 5.8°), gentle slope (15.6° ± 3.7°), and gentle yet rough terrain (16.8° ± 7.8°). Before estimating tree heights, the number of detected trees within each topographical feature was researched. In each of these terrains, we found that the percentage of trees detected correctly was 74, 86, and 92; the average error between LiDAR-derived and field measured tree heights was 0.227 m, -0.473 m, and -0.183 m; and the accuracy of the LiDAR-derived tree height estimates (RMSE: m) was 0.901 m, 0.846 m, and 0.576 m, respectively. Consequently, the procedure presented in this study could detect most canopy trees and estimate individual tree heights with an accuracy better than one meter, even in a forest with a mean slope angle of approximately 38°; thus, indicating that small-footprint airborne LiDAR will be a useful tool for accurately estimating the heights of individual canopy trees in sugi plantations in mountainous areas.

Furthermore, we investigated the possibility to estimate individual stem volumes in the sugi stands. In the research, we aim to (*i*) investigate which predictor variables with respect to crown properties,

derived from small-footprint airborne LiDAR data, together with LiDAR-derived tree height, could be useful in regression models to predict individual stem volumes, and (*ii*) to compare sum of predicted stem volumes for LiDAR-detected trees using the best regression model, with field-measured total stem volumes for all trees within stand. In the regression analysis, field-measured stem volumes were regressed against each of the six LiDAR-derived predictor variables with respect to crown properties, such as crown area, volume, and form, together with LiDAR-derived tree height. We found that the model with sunny crown mantle volume (*SCV*) had the smallest standard error of the estimate obtained from the regression model in each stand. The standard errors (m^3) were 0.144, 0.171, and 0.181 corresponding to 23.9%, 21.0%, and 20.6% of the average field-measured stem volume for detected trees in each of these stands, respectively. Furthermore, we found that sum of the individual stem volumes predicted by regression models with *SCV* for the detected trees, occupied 83-91% of field-measured total stem volumes within each stand, although 69-86% of the total number of trees was correctly detected by a segmentation procedure using LiDAR data.

All results of this study demonstrated that small-footprint airborne LiDAR is a useful and powerful tool for estimating many biophysical parameters accurately in both sugi and hinoki cypress stands in mountainous areas in Japan. We suggested that we should apply different methods for estimating them in sugi and hinoki cypress stands judging from the magnitude of laser penetration rates if we want to acquire the accurate estimates when using current small-footprint LiDAR systems. Although there will be room for improvement for the forest measurement system using small-footprint LiDAR presented in this study, especially for dense hinoki cypress stands, this study will provide a significant guideline for cross-checking of the accounted carbon stock and sink in FM activities under the Kyoto Protocol.

Keywords: *Chamaecyparis obtusa*, *Cryptomeria japonica*, DTM, mountaneous coniferous forest, LiDAR, remote sensing

摘　要

京都議定書に関わる炭素吸収量（3条3項、4項）の算定に、わが国では森林簿を中心とした行政データを用いることが検討されている（松本 2005）。しかし、森林簿については、その記載内容と現実との乖離がしばしば指摘されているように（森林・林業百科事典 2001）、現地での定期的な調査に代えて一定のモデルによって機械的に更新されている場合が多いため、森林簿の情報を基盤とした炭素吸収量算定値には不確実性が伴うことが予想される。京都議定書下では、算定のみならず、不確実性評価や検証といったQA/QC（品質保証/品質管理）により、その妥当性を示すことが求められているため、森林簿情報から算定される炭素吸収量推計値を「客観的かつ正確な方法」によって検証するシステムの構築が必要不可欠となる。

そのような客観的かつ正確な検証方法としてリモートセンシング技術が期待されているが、近年その高い測距精度および空間分解能で注目を集めている機器の中に、航空機LiDARと呼ばれる計測システムがある。航空機LiDARとは、航空機に搭載されたレーザー測距装置からレーザーパルスを照射し、反射点の物体の三次元（X, Y, Z）座標を計測する技術を指す。この技術の大きな特色は、他のリモートセンシング機器に比べ、物体の高さ計測の精度が十数センチと非常に高く、また、空中からは見え難い樹冠下の地表面の高さも計測できることにある。この技術にはsmall-footprint型と呼ばれる高空間分解能（数十cmオーダー）を有するものと、large-footprint型と呼ばれる低空間分解能（数十mオーダー）を有するものが存在するが、前者の機器が近年目覚しい技術進歩をとげ、欧米においては、針葉樹林を中心に林分レベルだけでなく、単木レベルの樹高、樹冠直径、胸高直径、立木幹材積など、炭素吸収量を評価する際に重要な因子の推定に関して、有用な結果が報告されている。したがって、日本の森林においても、small-footprint型航空機LiDAR（以下、LiDARと略す）が詳細かつ高精度な吸収源モニタリングに適用できるのであれば、時間と労力をかけることなく、また比較的広域かつ安定的に森林情報を取得できるため、炭素吸収量推計値のクロスチェックには有力な手法の一つとみなすことができる。

しかし、国内ではLiDARを用いた森林計測に関する詳細な研究例は、米ら（2002）の地形が平坦なカラマツ林での事例、及びOmasa *et al.*（2003）の地形が平坦でなおかつ立木密度の低いスギ林を対象にした事例のみである。京都議定書下で炭素吸収源の対象とみなされる可能性が高いのは、広葉樹林よりも成長が早い針葉樹人工林であり、特にわが国の森林面積の約40%、人工林面積の約67%を占めるスギ・ヒノキ人工林が大部分を占めるものと考えられるが、これら二つの報告だけでは吸収源モニタリングに対するLiDARの有用性が十分に示されたとは言いがたい。日本において、人工林の多くは、地形が急峻かつ複雑な地域に存在し、またその立木密度も先の報告のものより高い林分が多い。したがって、そのような現実的に評価の対象となるであろう地域及び林分状態においてもLiDARの森林計測能力が立証されなければ、この技術が炭素吸収量の推計値のクロスチェックに有効であるとは言えない。以上のことから、本研究では、LiDARによる森林計測の可能性を詳細に調べ、山岳地域の針葉樹人工林、特にスギ・ヒノキ人工林を対象としたLiDARよる森林計測システムを開発することを目的とした。

森林計測の対象となるパラメータの中で、特に重要視されるものは樹高である。樹高の成長は、林地の材積生産力や肥沃度を表す指標である地位と密接な関係があることが広く知られているが、その地位を査定するには正確な樹高値が必要とされる。また、樹高は炭素吸収量の推計に必要な立木幹材積や林分材積を推定するための有用なパラメータの一つでもある。しかし、現地調査により樹高を計測する場合、多大な労力および時間を要し、特に地形が急峻な場合は計測精度の低下も懸念される。したがって、山岳地域のスギ・ヒノキ人工林においてLiDARを用いて正確な樹高推定が可能かを明らかにすることは、LiDARよる森林計測手法の開発において最優先の課題となる。

これまでの研究例が示すように、LiDARによる樹高推定は、主に「レーザーパルスの一番目の反射波（FP）から算出する林冠表面の標高データ（DSM）」と、主に「レーザーパルスが樹冠を透過した後の最後の反射波（LP）から算出する地表面の標高データ（DTM）」との差分をとることによりその推定が可能

となる。すなわち、樹高推定精度はDSMおよびDTMの両者の計測(推定)精度に依存する。DSMはLiDARによって林冠表面の三次元座標を数十cmレベルで直接計測したデータを主に使用して構築されるため、DSMの精度は非常に高いものとみなすことができる。一方、DTMは、LiDARから照射したレーザーパルスが樹冠を透過し、地表面にまで到達した反射データを使用して構築されるため、レーザーパルスの樹冠透過率(すなわち地表面データの捕捉率)がDTMの推定精度に大きくかかわることとなる。

そこで第二章では、樹高の推定の可能性を検証するため、山岳地域の開空度が等しい樹冠閉鎖した壮齢スギ・ヒノキ林分を対象として、LiDARのレーザーパルスの樹冠透過率を詳細に検討した。その結果、レーザーパルスの樹冠透過率(P_{t+s})は、スギ林分では8.1%(そのうち、FP透過率(P_f)が2.6%、SP(上記のLPとほぼ同意)透過率(P_s)が5.5%)、ヒノキ林分では1.1%(そのうち、FP透過率が0.1%、SP透過率が1.1%)であることがわかった。この透過率に対し、母比率の差の検定をおこなったところ、両林分間で全ての透過率(P_{t+s}, P_t, P_s)に有意な差($p<0.001$)が認められた。このことから、山岳地域の壮齢スギ林分に比べ、山岳地域の壮齢ヒノキ林分ではDTMを構築するために必要な地表面データが非常に少なく、そのデータのみから精度の高いDTMを構築するのは困難である可能性が示唆された。

さらに、第二章の結果から、ヒノキ林分においては樹高推定を試みたとしても、精度の高い樹高推定の可能性は低いと考えられた。特にヒノキ林分においては、LiDARから得られる三次元位置座標データ(以下、LiDARデータと称す)は林冠表層部に集中していることから、第三章では樹冠に関わる変数を用い、樹高に代わる有用な森林計測パラメータの推定について検討した。そこで、陽樹冠着葉部の体積が樹木の幹材積成長量を示す指標として有用であるとの報告(梶原 1984)から、LiDARデータのみから算出可能な陽樹冠着葉部体積を用い、林分材積の推定の可能性について検討した。東京大学愛知演習林内の72年生および16年生のヒノキ林分に合計8プロットを設置し、実測によるプロット内の林分材積(V)と、LiDARデータによるプロット内の推定陽樹冠着葉部体積の合計値(V_{ss3})の関係について、回帰分析を用いて調べたところ、決定係数が0.922($p<0.01$)という高い相関の回帰式($V=0.0379V_{ss3}$)が得られた。このことから、得られた回帰式の普遍性についてはさらに検討が必要と考えられるが、少なくともLiDARデータのみから算出可能なV_{ss3}は、林分材積を高精度に推定するための有用な変数であることが示唆された。

次に、第二章の結果から、スギ林分においてはヒノキ林分と比較して精度の良いDTMの構築の可能性が考えられたため、第四章(4a)においてはスギ人工林を対象として、LiDARデータによる樹高の推定精度、及び林地の地形がその推定精度に及ぼす影響について詳細に検討した。本研究科附属演習林内の48年生スギ林分を対象に、同一林分内を地形及び傾斜の特徴別にsteep slope(平均±標準偏差;37.6±5.8度)、gentle slope(15.6±3.7度)、gentle yet rough terrain(16.8±7.8度)の3サイトにわけ、それぞれのサイトごとに全立木の実測樹高とLiDARデータによる推定樹高の関係を回帰分析により調べた。その結果、全てのサイトにおいて、回帰式の傾きは有意に1とみなされ($p<0.01$)、また、切片は0との間に有意差が認められなかった($p>0.05$)。また、樹高推定精度はRMSE(平均二乗誤差の平方根)で先のサイト順に0.901m、0.846m、0.576mであった。これらの結果から、平均傾斜角約38度ほどのスギ林分であっても、LiDARにより、1m以下の精度で樹高推定が可能であることが示唆された。

最後に、第四章(4b)では、先の第四章(4a)と同じ3サイトにおいて、単木の立木幹材積及び林分材積推定精度について検討した。この章では、(i) LiDARデータから得られる樹冠に関する独立変数の中で、どの独立変数がLiDARによる推定樹高と共に立木幹材積予測の線形回帰モデルに有用であるか、及び(ii) LiDARで検出できた樹木に対し、最良の線形回帰モデルから予測した単木材積を合計した場合の林分材積推定値を、第四章(4a)と同様に林地の地形が及ぼす影響も含め検討した。まず(i)に関しては、樹冠面積、樹冠体積、樹冠形等の樹冠に関する6つの変数と共に、第四章(4a)で得られた推定樹高も独立変数として、実測の立木幹材積を目的変数とする重回帰分析を行った。その結果、全てのサイトにおいて、第三章で着目した陽樹冠着葉部体積(SCV)を変数にもつモデルの標準誤差が最も小さいことが示された。その誤差は、先のサイトの順に0.112 m^3、0.171 m^3、0.181 m^3で、これは検出木の平均立木幹材積の18.7%、21.0%、20.6%にそれぞれあたった。次に(ii)に関しては、各サイトにおける樹木の本数検出率が70%から85%であったのに対し、SCVの回帰モデルで予測した検出木の単木材積の合計は、真の林分材積の80%から90%を占めることがわかった。

以上の結果から、以下にLiDARを用いた日本の山岳地域針葉樹人工林における森林計測システムを提案する。まず、レーザーパルスの樹冠透過率を計算し、精度の良い樹高推定を可能にするDTMの構築の可否を判断する。その際の透過率の目安としては、本研究で示した値である8%程度を基準とし、それ以上である場合においては高精度の樹高推定が可能であると考えられるため、第四章で提案した樹高推定、立木幹材積推定、ならびに林分材積推定手法を用いる。それぞれの推定精度は本研究で示された程度のものが期待できると考えられる。一方、本研究で明らかにしたとおり、ヒノキ林分のように、レーザーパルスの樹冠透過率が1%程度の場合は、現状では樹高推定を避け、第三章で示した推定陽樹冠着葉部体積の合計値(V_{ss3})を用いて林分材積推定を行う。以上のように、本研究で提案したsmall-footprint型航空機LiDARによる山岳地域針葉樹林の森林計測システムは、特に過密なヒノキ林分での方法論に関して改善の余地はあるが、本研究は京都議定書下の森林経営における炭素吸収量推計値のクロスチェックの方法に対し、一つの重要な指針を与えるだろう。

キーワード:山岳地域針葉樹人工林,スギ,ヒノキ,Li-DAR,リモートセンシング,DTM,レーザーパルス